5-17-2018

Provenance and Paleogeography of the 25-17 Ma Rainbow Gardens Formation: Evidence for Tectonic Activity at Ca. 19 Ma and Internal Drainage rather than Throughgoing Paleorivers on the Southwestern Colorado Plateau

Melissa A. Lamb
Univesrity of St. Thomas

L. Sue Beard
U.S. Geological Survey

Malia Dragos
University of St. Thomas

Andrew D. Hanson
University of Nevada, Las Vegas, andrew.hanson@unlv.edu

Thomas A. Hickson
University of St. Thomas

See next page for additional authors

Repository Citation

Lamb, M. A., Beard, L. S., Dragos, M., Hanson, A. D., Hickson, T. A., Sitton, M., Umhoefer, P. J., Karlstrom, K. E., Dunbar, N., McIntosh, W. (2018). Provenance and Paleogeography of the 25-17 Ma Rainbow Gardens Formation: Evidence for Tectonic Activity at Ca. 19 Ma and Internal Drainage rather than Throughgoing Paleorivers on the Southwestern Colorado Plateau. *Geosphere, 14*(4), 1592-1617.
http://dx.doi.org/10.1130/GES01127.1

Authors
Melissa A. Lamb, L. Sue Beard, Malia Dragos, Andrew D. Hanson, Thomas A. Hickson, Mark Sitton, Paul J. Umhoefer, Karl E. Karlstrom, Nelia Dunbar, and William McIntosh

GEOSPHERE

GEOSPHERE; v. 14, no. 4

https://doi.org/10.1130/GES01127.1

10 figures; 2 tables; 1 set of supplemental files

CORRESPONDENCE: malamb@stthomas.edu

CITATION: Lamb, M.A., Beard, L.S., Dragos, M., Hanson, A.D., Hickson, T.A., Sitton, M., Umhoefer, P.J., Karlstrom, K.E., Dunbar, N., and McIntosh, W., 2018, Provenance and paleogeography of the 25–17 Ma Rainbow Gardens Formation: Evidence for tectonic activity at ca. 19 Ma and internal drainage rather than throughgoing paleorivers on the southwestern Colorado Plateau: Geosphere, v. 14, no. 4, p. 1592–1617, https://doi.org/10.1130/GES01127.1.

Science Editor: Raymond M. Russo
Guest Associate Editor: Andres Aslan

Received 3 September 2014
Revision received 11 January 2018
Accepted 16 March 2018
Published online 17 May 2018

Provenance and paleogeography of the 25–17 Ma Rainbow Gardens Formation: Evidence for tectonic activity at ca. 19 Ma and internal drainage rather than throughgoing paleorivers on the southwestern Colorado Plateau

Melissa A. Lamb[1], L. Sue Beard[2], Malia Dragos[1], Andrew D. Hanson[3], Thomas A. Hickson[1], Mark Sitton[4], Paul J. Umhoefer[4], Karl E. Karlstrom[5], Nelia Dunbar[6], and William McIntosh[6]

[1]Department of Geology OWS 153, University of St. Thomas, 2115 Summit Avenue, St. Paul, Minnesota 55105, USA
[2]U.S. Geological Survey, 2255 N. Gemini Drive, Flagstaff, Arizona 86001, USA
[3]Geoscience Department, University of Nevada–Las Vegas, Las Vegas, Nevada 89154, USA
[4]School of Earth Sciences & Environmental Sustainability, Northern Arizona University, 625 S. Knoles Drive, Flagstaff, Arizona 86011, USA
[5]Department of Earth and Planetary Sciences, 1 University of New Mexico, MSC03 2040, Albuquerque, New Mexico 87131-0001, USA
[6]New Mexico Bureau of Geology & Mineral Resources *and* Earth and Environmental Science Department, New Mexico Tech, Socorro, New Mexico 87801, USA

ABSTRACT

The paleogeographic evolution of the Lake Mead region of southern Nevada and northwest Arizona is crucial to understanding the geologic history of the U.S. Southwest, including the evolution of the Colorado Plateau and formation of the Grand Canyon. The ca. 25–17 Ma Rainbow Gardens Formation in the Lake Mead region, the informally named, roughly coeval Jean Conglomerate, and the ca. 24–19 Ma Buck and Doe Conglomerate southeast of Lake Mead hold the only stratigraphic evidence for the Cenozoic pre-extensional geology and paleogeography of this area. Building on prior work, we present new sedimentologic and stratigraphic data, including sandstone provenance and detrital zircon data, to create a more detailed paleogeographic picture of the Lake Mead, Grand Wash Trough, and Hualapai Plateau region from 25 to 18 Ma. These data confirm that sediment was sourced primarily from Paleozoic strata exposed in surrounding Sevier and Laramide uplifts and active volcanic fields to the north. In addition, a distinctive signal of coarse sediment derived from Proterozoic crystalline basement first appeared in the southwestern corner of the basin ca. 25 Ma at the beginning of Rainbow Gardens Formation deposition and then prograded north and east ca. 19 Ma across the southern half of the basin. Regional thermochronologic data suggest that Cretaceous deposits likely blanketed the Lake Mead region by the end of Sevier thrusting. Post-Laramide northward cliff retreat off the Kingman/Mogollon uplifts left a stepped erosion surface with progressively younger strata preserved northward, on which Rainbow Gardens Formation strata were deposited. Deposition of the Rainbow Gardens Formation in general and the 19 Ma progradational pulse in particular may reflect tectonic uplift events just prior to onset of rapid extension at 17 Ma, as supported by both thermochronology and sedimentary data. Data presented here negate the California and Arizona River hypotheses for an "old" Grand Canyon and also negate models wherein the Rainbow Gardens Formation was the depocenter for a 25–18 Ma Little Colorado paleoriver flowing west through East Kaibab paleocanyons. Instead, provenance and paleocurrent data suggest local to regional sources for deposition of the Rainbow Gardens Formation atop a stripped low-relief western Colorado Plateau surface and preclude any significant input from a regional throughgoing paleoriver entering the basin from the east or northeast.

INTRODUCTION

The Lake Mead region (Figs. 1 and 2) contains the eastern limit of Sevier thrusting and the eastern portion of central Basin and Range extension of Miocene age. Situated north of the Colorado River extensional corridor, west of the Colorado Plateau and Grand Canyon, and south of the northern Basin and Range (central Nevada), the geology of the Lake Mead region is well poised to inform tectonic models of extension as well as regional paleogeographic reconstructions and landscape evolution models. Sedimentary deposits of the ca. 25 Ma to ca. 17 Ma late Oligocene–early Miocene Rainbow Gardens Formation east of Las Vegas—formerly the lowest member of the Horse Spring Formation—have been interpreted as predating the onset of extension in the central Basin and Range, whereas the younger Horse Spring Formation records the main phase of extension from ca. 17 to 12 Ma (Bohannon, 1984; Beard, 1996; Lamb et al., 2005). Lamb et al. (2015) presented sedimentologic, stratigraphic, geochronologic, isotopic, and geochemical data to reconstruct the Rainbow Gardens Formation basin and its paleogeography throughout its formation and evolution. They concluded that the basin formed prior to extension and received sediment from local Paleozoic and Mesozoic units, as well as volcanic input from the Caliente and Kane Wash volcanic centers to the north.

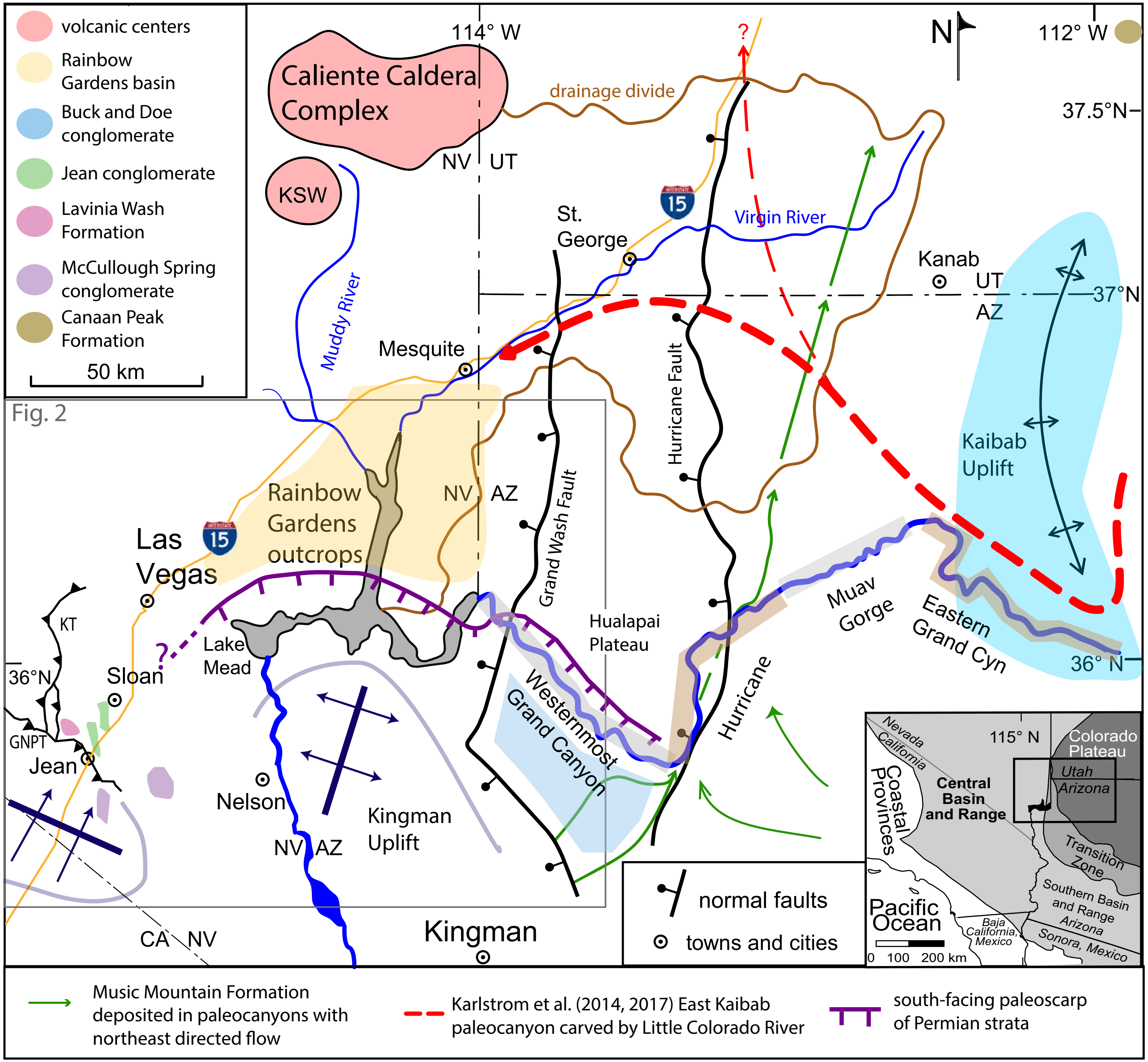

Figure 1. Map of the Lake Mead and Grand Canyon area, modified from Dickinson et al. (2014) and Karlstrom et al. (2014). Bold blue line marks the Colorado River; other blue lines are tributaries; brown line delineates Virgin River drainage; dashed black lines indicate state boundaries (AZ—Arizona, CA—California, NV—Nevada, UT—Utah). Green lines show location of the 65–55 Ma Music Mountain Formation (MFF) and associated sediment transport directions; note that this formation was deposited within paleocanyons and thus crops outs as lines. Gray and light brown bars show segments of the Grand Canyon named by Karlstrom et al. (2014). Inset map in lower right shows location of Figure 1 on a map of southwestern U.S. physiographic provinces (modified from Wernicke et al., 1988; Stewart, 1998). Gray box shows the location of Figure 2. GNPT—Gerstley-Nopah Peak thrust fault; KT—Keystone thrust; KSW—Kane Springs Wash.

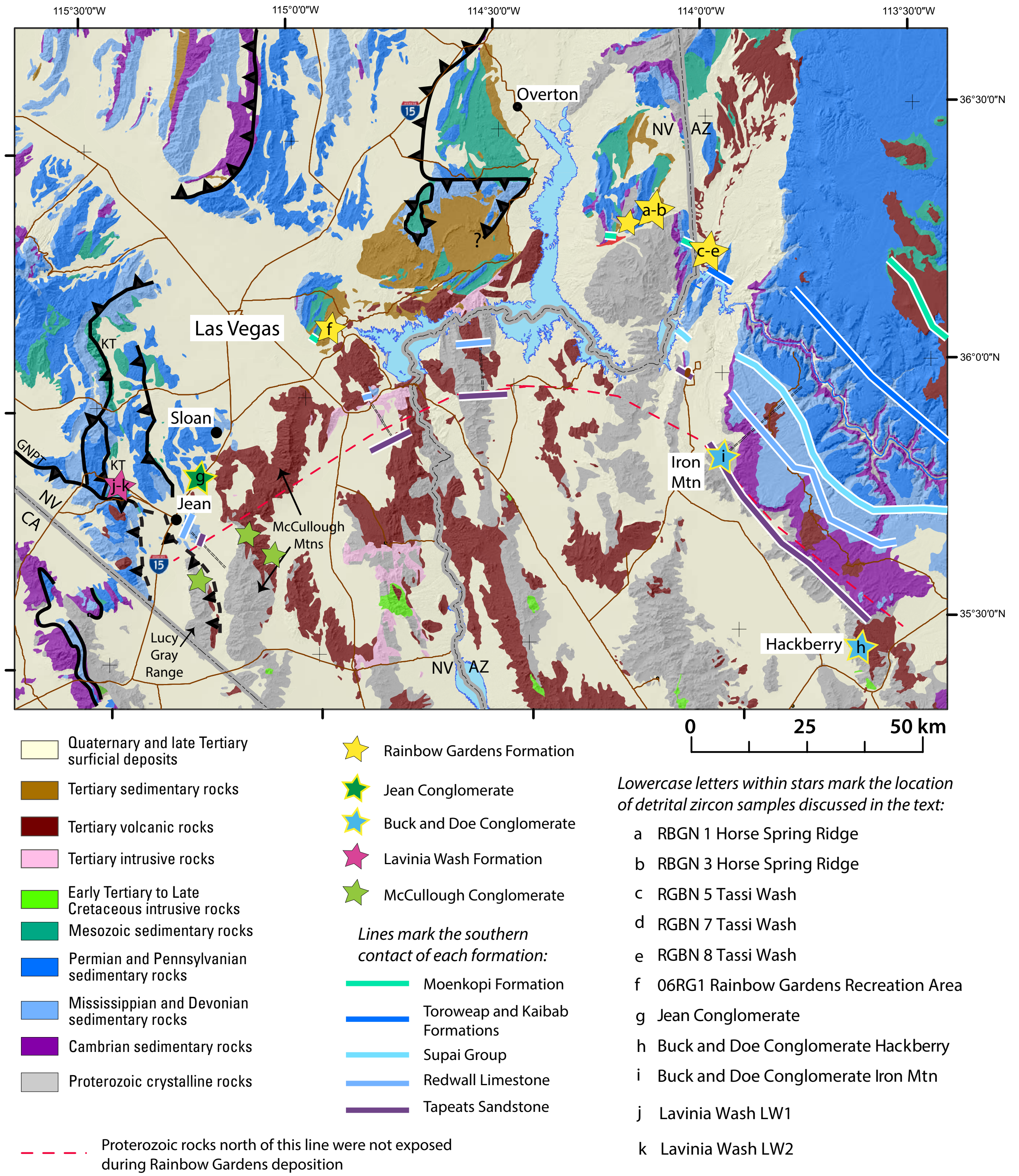

Figure 2. Geologic map of the Lake Mead area, northern Colorado River extensional corridor and southwestern Colorado Plateau. Base map is from Ludington et al. (2007). GNPT—Gerstley-Nopah Peak thrust fault of Pavlis et al. (2014); KT—Keystone thrust. The hypothesized dashed southeasterly extensions of the Gerstley–Nopah Peak thrust are ours, not Pavlis et al. (2014). Colored lines are generalized southern contacts of strata on post-Laramide, pre-extension erosion surface (sub–Rainbow Gardens Formation unconformity; Beard and Faulds, 2011). Yellow stars include the Rainbow Gardens Formation (the four stars north of Lake Mead and east of Las Vegas), the Jean Conglomerate, and, in the southeast, the Buck and Doe Conglomerate at Iron Mountain and Hackberry locations.

They hypothesized that the southern part of the basin may contain a record of an earlier onset of extension or uplift related to volcanism south of Lake Mead. For this study, we had three goals: (1) to better define the paleogeography of the southern part of the basin and surrounding region, (2) to test the hypothesis of Lamb et al. (2015) that extension began in the southeastern Lake Mead region by ca. 19 Ma and may have created an unconformity within the Rainbow Gardens Formation, and (3) to further examine how the Rainbow Gardens Formation stratigraphic record informs the formation of the Grand Canyon debate and test the hypothesis that the Rainbow Gardens Formation basin was a sink for Little Colorado paleoriver sediment (Fig. 1; Karlstrom et al., 2014).

Goal 1: Better Define the Paleogeography of the Southern Part of the Basin and Surrounding Region

Lamb et al. (2015) determined that the Rainbow Gardens Formation basin began as an east-northeast–trending valley formed by the inherited topography of Sevier and Laramide highlands to the north, west, and south and a subtle, low-relief boundary to the east. They concluded that, for much of the Cenozoic, the valley was a zone of bypass to the northeast for sediment eroded off the nearby topographic highs, but that uplift to the northeast triggered the initiation of deposition of sediment around 26 Ma, as first suggested by Beard (1996). Lamb et al. (2015) presented paleogeographic diagrams showing the basin configuration and focused on the basin fill (their figures 12 and 13), including the deposition of fluvial volcaniclastic sediments from the volcanic fields to the northeast. They also indicated that the nature of southwest margin was obscure (their figure 12).

Goal 2: Test the Hypothesis that Extension Began in the Southern Lake Mead Region by ca. 19 Ma

Lamb et al. (2015) hypothesized that the southern margin of the Rainbow Gardens Formation basin might contain a previously unrecognized unconformity that could signify uplift to the south and/or an earlier start to extension, around 19 Ma. They cited the abrupt progradation of coarse clastics into the basin during the middle of Rainbow Gardens Formation deposition, at ca. 19 Ma, as well as an apparent thinning to the south of a stratigraphic package immediately above this coarse unit, during the latter half of deposition, as evidence of a possible earlier start to extension. Thermochronologic data may support this idea, as these data indicate cooling related to tectonic exhumation was clearly under way by ca. 17 Ma in the eastern Lake Mead area, but may have begun at 20–19 Ma (e.g., Fitzgerald et al., 1991, 2009; Reiners et al., 2000; Quigley et al., 2010). Fitzgerald et al. (2009) documented a thermal history for the Gold Butte and White Hills area that begins with Laramide cooling starting ca. 75 Ma and transitions to rapid cooling beginning ca. 17 Ma at Gold Butte and at 18 Ma in the White Hills. Because these dates reflect cooling through the partial annealing zone, Fitzgerald et al. (2009) indicated that the ages may underestimate the onset of cooling by 1–2 m.y. or more, meaning cooling could have begun ca. 20–19 Ma. Quigley et al. (2010) found that apatite fission-track ages and track length measurements revealed a transition from slow cooling beginning 30–26 Ma to rapid cooling at ca. 17 Ma.

Goal 3: Examine How the Rainbow Gardens Formation Stratigraphic Record Informs the Debate about the Formation of the Grand Canyon

Karlstrom et al. (2013) summarized generally accepted ideas on the evolution and integration of the Colorado River system and enumerated the many specific controversies related to the Colorado River and carving of the Grand Canyon and (e.g., Wernicke, 2011; Flowers et al., 2008; Flowers and Farley, 2012; Karlstrom et al., 2013, 2014; Lee et al., 2013). Most researchers agree that during the Late Cretaceous and Early Cenozoic, rivers, sourced from Laramide uplifts, flowed north and northeast across the Colorado Plateau and may have flowed along Laramide fault-bounded uplifts (Karlstrom et al., 2014), and along the front of the Sevier thrust belt (Dickinson et al., 2012), possibly to depocenters in the Uinta basins (Davis et al., 2010). During this time, the southwestern Colorado Plateau was beveled into a complex erosion surface, where Paleozoic units dipped north with NW-striking contacts (Fig. 2). Regional base level and periodic aggradation on the Hualapai Plateau from the time of the 65–55 Ma Music Mountain Formation through the 24–19 Ma Buck and Doe Formation, to younger than ca. 19 Ma (Coyote Springs Formation), have been cited as incompatible with any deep paleocanyon of near-modern depth during this time (Young and Crow, 2014). Establishment of the modern southwest-flowing Colorado River by 6–5 Ma is supported by many workers (e.g., Young 1979, 1999, 2001; Young and Hartman, 2014; Winn et al., 2017). Karlstrom et al. (2014) discussed the five separate segments of the modern Grand Canyon (Fig. 1) and concluded that the westernmost Grand Canyon segment, closest to Lake Mead, formed after 6 Ma. They (and Lee et al., 2013) suggested that the eastern Grand Canyon segment was partially carved across the Kaibab Plateau between 25 and 15 Ma, likely by the paleo–Little Colorado River (Karlstrom et al., 2017), which then flowed northwest and deposited sediment into the Lake Mead area basins from the north (Fig. 1). If so, deposits of the pre-and synextensional basins should contain evidence of derivation from distal parts of the Colorado Plateau. The Lake Mead region lies immediately adjacent to the mouth of the Grand Canyon where it emerges from the Colorado Plateau (Figs. 1 and 2), and river incision has exposed pre- and synextensional basin sediments that bracket much of the time involved in the Grand Canyon controversy (e.g., Pederson, 2008). Thus, these basins are well positioned to test the hypothesis that the Lake Mead region was a sump for sediment originating from a river that carved the eastern Grand Canyon segment during the Miocene and emptied into the Rainbow Gardens Formation basin from the northeast (e.g., Karlstrom et al., 2014, 2017; Figs. 1 and 2). Lamb et al. (2015) concluded that Colorado Plateau paleorivers did not empty into the Lake Mead region ca. 25–18 Ma, based on stratigraphic correlations, paleocurrent data, and detailed facies documentation, and we support and build on that work here.

In this study, we present new sandstone provenance and stratigraphic data as well as detrital zircon analyses from the Rainbow Gardens Formation and correlative Oligocene–Miocene units to the south of Lake Mead to address these goals. We better define the southern basin configuration and sediment source and pathways of the Rainbow Gardens Formation, further address the time of initiation of extension, and further test the hypothesis that the Rainbow Gardens Formation basin was a possible sink for Little Colorado paleoriver sediment between 25 and 17 Ma.

BACKGROUND GEOLOGY

The Lake Mead region records several major events within the complex geologic history of the U.S. Southwest. Proterozoic crystalline basement, i.e., plutonic and metamorphic rocks, exposed south of Lake Mead record the suture between the Mojave and Yavapai crustal provinces and the growth of the continent (Fig. 2; Bennett and DePaolo, 1987; Duebendorfer et al., 2001). Paleozoic sedimentary units that thicken toward the west from the Grand Canyon to west of Las Vegas record passive-margin deposition, whereas Mesozoic strata mark the transition to a nonmarine setting (e.g., Beard et al., 2007). Cretaceous Sevier thrusting north and west of Lake Mead subsequently placed Paleozoic carbonates over Mesozoic rocks (e.g., Wernicke et al., 1988). Laramide deformation produced the Kingman Uplift (originally called the Kingman Arch) south of Lake Mead and west of the Colorado Plateau (Figs. 1 and 2; Bohannon, 1984; Faulds et al., 2001; Beard and Faulds, 2011), roughly coincident spatially with the Miocene northern Colorado River extensional corridor. These Mesozoic and early Cenozoic contractional events created highlands in the Lake Mead and Lower Colorado River area, with river systems that flowed northeast and carved canyons across what is now the Grand Canyon region (Young and Hartman, 2014; Young and Crow, 2014). Contraction was followed by a period of tectonic quiescence and erosion that stripped much of the Paleozoic and Mesozoic strata. South of Lake Mead, these Phanerozoic deposits were completely eroded from the Kingman Uplift, exposing Proterozoic basement, and sediment derived from this erosion was deposited across the southwestern Colorado Plateau (Young, 1999). These deposits are preserved in paleocanyons as the Paleocene–Eocene Music Mountain Formation (Fig. 1; Young, 1999; Young and Hartman, 2014; Young and Crow, 2014). Although similar drainage systems may have also flowed northeast across the Lake Mead region and into southwest Utah, there is no Paleocene–Eocene stratigraphic record.

On the north and east flanks of the Kingman Uplift, erosion created a fairly low-relief, beveled surface across gently north- and northeast-dipping Paleozoic and Mesozoic strata (Bohannon, 1984) with one notable exception. A distinctive paleotopographic barrier resulted from a south- to southwest-facing scarp (hachured line on Fig. 1) formed by the resistant Permian Kaibab and Toroweap Formations. This escarpment retreated north and northeast by undercutting of the soft, underlying Permian Hermit Formation (e.g., Lucchitta, 1966; Young, 1985, Lucchitta and Young, 1986; Beard, 1996; Faulds et al., 2001).

The latest Oligocene to early Miocene transition from tectonic quiescence to extension included volcanic activity to the north and south of the Lake Mead region, with concomitant deposition of sedimentary units, the first preserved in the Lake Mead region after the long period of erosion. To the north of the Lake Mead region, the Caliente caldera complex produced several major silicic eruptions from 24 to 18.5 Ma (Fig. 1; Best et al., 2013). To the south, volcanism began around 22 Ma (south of Kingman in Fig. 1) and migrated northward through time (Faulds et al., 2001). The Rainbow Gardens Formation, along the north flank of the uplift, extends from the Rainbow Gardens Recreation Area east of Las Vegas to just east of the Nevada-Arizona border (Figs. 1–3; Bohannon, 1984; Beard, 1996; Lamb et al., 2015). The deposits are only found north of the Permian escarpment that retreated off the Kingman Uplift and only on rocks of Permian age and younger. They contain volcanic tuffs and detritus from the Caliente volcanic field that help bracket its age between ca. 25 to ca. 18 Ma, but it may be as young at ca. 17 Ma (Beard, 1996; Umhoefer et al., 2010). The Rainbow Gardens Formation (Fig. 3) records basin filling that is similar throughout its outcrop belt. It includes a basal clast-supported alluvial conglomerate (Trc), a mixed-lithology middle unit (Trm), which includes fluvial siliciclastics as well as palustrine and lacustrine carbonate and evaporite deposits, and a capping resistant carbonate unit (Trl) that principally is composed of massive limestone beds formed in shallow lakes and marshy environments (Fig. 3).

Oligocene–Lower Miocene sedimentary rocks south of Lake Mead are dominantly alluvial sandstones and conglomerate. These southern deposits also predate extension, were likely deposited across the Kingman Uplift, and are now preserved only on its flanks. They include (1) the Jean Conglomerate (Hanson, 2008) and other nearby conglomeratic units in unconformable contact on the Pennsylvanian–Permian Bird Spring Formation (House et al., 2006; Garside et al., 2012; Hinz et al., 2015), (2) the McCullough Spring Conglomerate in the McCullough Mountains and Lucy Gray Range (Herrington, 1993), (3) various arkosic sandstones and conglomerates (informally called "the basal arkose") in the interior part of the Kingman Uplift south of Lake Mead (e.g., Anderson, 1978; Faulds, 1996; Faulds et al., 2001), and (4) the Buck and Doe Conglomerate along the western margin of the Colorado Plateau to the east of the uplift (Young and Crow, 2014). The Buck and Doe Conglomerate contains a 24 Ma tuff (Young and Crow, 2014); the other deposits are only bracketed by overlying ca. 20 Ma to 18.5 Ma Miocene volcanic rocks.

According to Faulds et al. (2001), east-west extension that formed the northern Colorado River extensional corridor followed inception of magmatism by 1–4 m.y., with the peak of extension migrating northward toward Lake Mead from ca. 16.5 to 15.5 Ma. They suggested mild north-south extension between ca. 20 and 16 Ma that preceded the main period of extension and attributed this to southerly collapse of the remnant Kingman Uplift topography into the northward-migrating extensional terrane. Major east-west extension in the Lake Mead area began ca. 17 Ma, peaked ca. 15 Ma, and continued until at least 10 Ma.

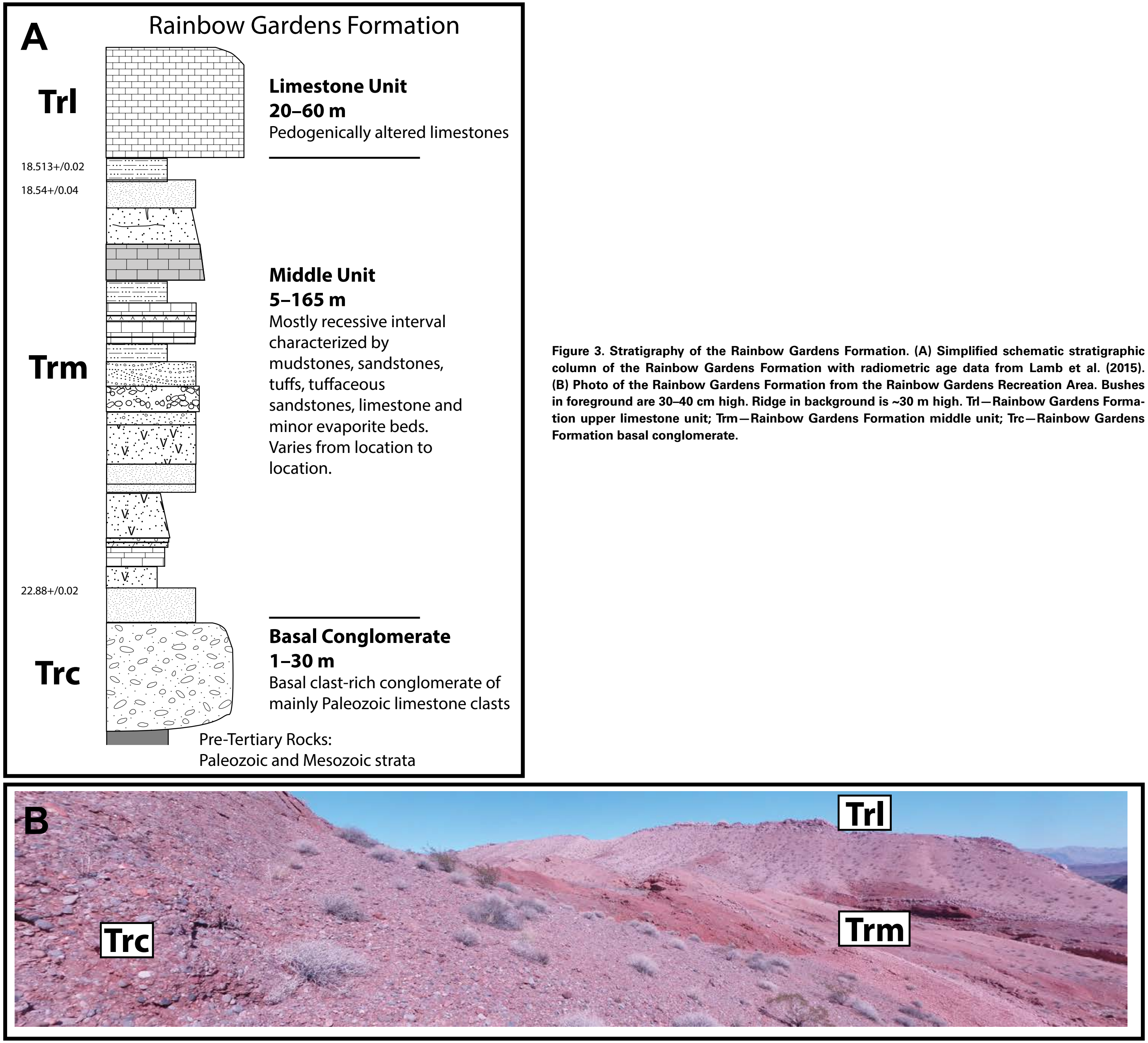

Figure 3. Stratigraphy of the Rainbow Gardens Formation. (A) Simplified schematic stratigraphic column of the Rainbow Gardens Formation with radiometric age data from Lamb et al. (2015). (B) Photo of the Rainbow Gardens Formation from the Rainbow Gardens Recreation Area. Bushes in foreground are 30–40 cm high. Ridge in background is ~30 m high. Trl—Rainbow Gardens Formation upper limestone unit; Trm—Rainbow Gardens Formation middle unit; Trc—Rainbow Gardens Formation basal conglomerate.

This foundering of the central Basin and Range relative to the adjacent Colorado Plateau resulted in the development of numerous basins (e.g., Wernicke et al., 1988; Duebendorfer et al., 1998; Fryxell and Duebendorfer, 2005; Umhoefer et al., 2010). Filling of extensional basins is recorded by the 17 Ma to 13 Ma Horse Spring Formation (Bohannon, 1984; Beard, 1996; Lamb et al., 2005). The Muddy Creek Formation, and the informal red sandstone and Tertiary–Quaternary alluvial deposits (e.g., Bohannon, 1984; Beard et al., 2007) overlie the Horse Spring Formation.

METHODS

In this paper, we examined the southern portion of the Rainbow Gardens Formation basin by focusing on the stratigraphy of three north-to-south transects. We present 11 detailed stratigraphic sections, four of which were previously presented in Lamb et al. (2015), as well as conglomerate composition and paleocurrent data. In order to reconstruct the Rainbow Gardens Formation basin paleogeography, we use a map of reconstructed fault blocks from Lamb et al. (2015) to show the relative locations of our measured sections and samples (Fig. 4; for a more complete discussion of retrodeformation of these highly simplified blocks and the entire Rainbow Gardens Formation basin reconstruction, see Lamb et al., 2015). To characterize variations in sandstone composition through time, we examined over 97 thin sections and point counted 23 sandstones from the 10 measured sections in the southern part of the basin. Some samples were very poorly sorted, and our point counts used a grid spacing that was larger than the estimated mean grain size. This means larger grains were typically counted more than once, thus capturing their contribution to the overall composition. Finally, we present 11 detrital zircon analyses from seven locations (five samples also presented in Crossey et al., 2015). Detrital zircon analyses were completed at the University of Arizona laboratory (Supplemental File S1[1]). Using the methods of Dickinson and Gehrels (2009), we used the detrital zircon data to calculate a maximum depositional age for each sample to support the stratigraphic and geochronologic data. We calculated maximum depositional ages using techniques from Dickinson and Gehrels (2009), including the youngest single grain (YSG), the youngest from probability plot (YPP), the youngest 1σ grain cluster (YC1σ), and youngest 2σ grain cluster (YC2σ) methods.

RESULTS

Stratigraphy and Facies Changes

The Rainbow Gardens Formation contains lateral and vertical variations in composition that can be used to interpret basin geometry, fill, provenance, and paleogeography. Here, we focused on the southern half of the basin from Frenchman Mountain at the Rainbow Gardens Recreation Area near Las Vegas to the Grand Wash Trough (Tassi Wash). Figures 5A and 5B show north-south

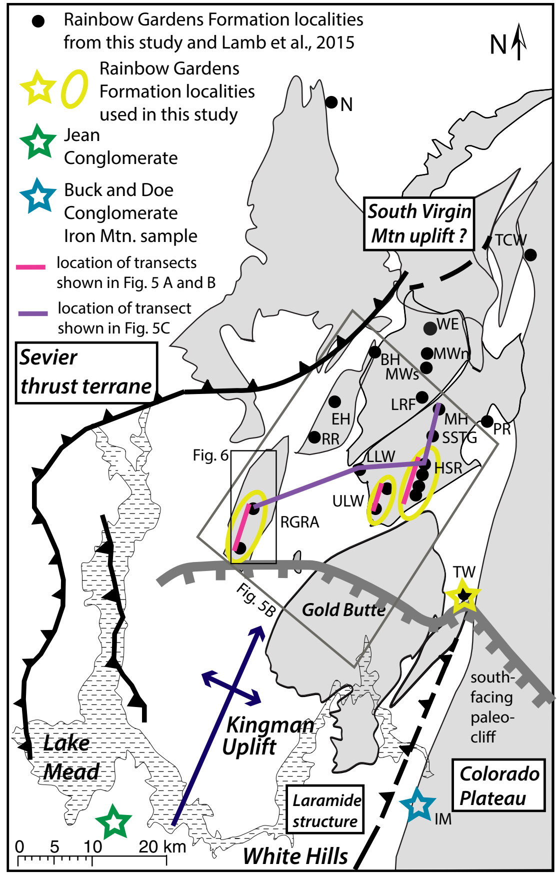

Figure 4. Reconstructed Miocene paleogeography: gray shading represents fault blocks shown in a pre-extension, retrodeformed configuration from Lamb et al. (2015) with the modern features of the Colorado Plateau, White Hills, and Lake Mead for visual reference. Key Miocene features present during deposition of the Rainbow Gardens Formation, including the Sevier thrust terranes, Kingman Uplift, and south-facing paleocliff of Permian strata, are also shown. The Kingman Uplift is a north-plunging, broad antiformal dome. Ovals and stars highlight locations of outcrops of Rainbow Gardens Formation and correlative units, with new data presented in this paper. Note that only one of two Buck and Doe Conglomerate sample localities, the Iron Mountain sample, is shown on this map: the other one, Hackberry, is farther south, as shown on Figure 2. Black dots represent measured sections presented here and in Lamb et al. (2015). Diagonal box shows the location of the base map used in Figure 5B fence diagram. Inset rectangular box shows location of image used in Figure 6. Locality name abbreviations: BH—Boathouse Cove; EH—Echo Hills; HSR—Horse Spring Ridge; IM—Iron Mountain, LRF—Lime Ridge fault; LLW—lower Lime Wash; MH—Mud Hills; MWn—Mud Wash north; MWs—Mud Wash south; N—Narrows; PR—Pakoon Ridge; RGRA—Rainbow Gardens Recreation Area; RR—Razorback Ridge; SSTG—south St. Thomas Gap; TCW—Tom and Cull Wash; TW—Tassi Wash; ULW—upper Lime Wash; WE—Wechech.

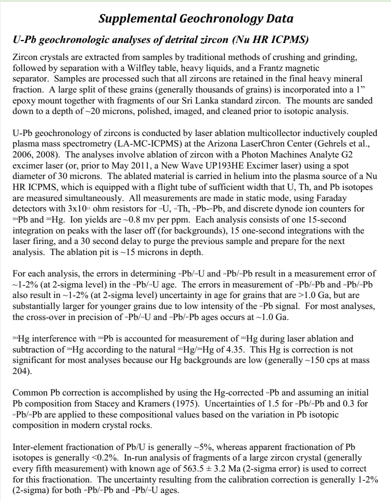

Supplemental Geochronology Data

U-Pb geochronologic analyses of detrital zircon (Nu HR ICPMS)

Zircon crystals are extracted from samples by traditional methods of crushing and grinding, followed by separation with a Wilfley table, heavy liquids, and a Frantz magnetic separator. Samples are processed such that all zircons are retained in the final heavy mineral fraction. A large split of these grains (generally thousands of grains) is incorporated into a 1" epoxy mount together with fragments of our Sri Lanka standard zircon. The mounts are sanded down to a depth of ~20 microns, polished, imaged, and cleaned prior to isotopic analysis.

U-Pb geochronology of zircons is conducted by laser ablation multicollector inductively coupled plasma mass spectrometry (LA-MC-ICPMS) at the Arizona LaserChron Center (Gehrels et al., 2006, 2008). The analyses involve ablation of zircon with a Photon Machines Analyte G2 excimer laser (or, prior to May 2011, a New Wave UP193HE Excimer laser) using a spot diameter of 30 microns. The ablated material is carried in helium into the plasma source of a Nu HR ICPMS, which is equipped with a flight tube of sufficient width that U, Th, and Pb isotopes are measured simultaneously. All measurements are made in static mode, using Faraday detectors with $3x10^{11}$ ohm resistors for U, Th, Pb–Pb, and discrete dynode ion counters for ^{204}Pb and ^{202}Hg. Ion yields are ~0.8 mv per ppm. Each analysis consists of one 15-second integration on peaks with the laser off (for backgrounds), 15 one-second integrations with the laser firing, and a 30 second delay to purge the previous sample and prepare for the next analysis. The ablation pit is ~15 microns in depth.

For each analysis, the errors in determining Pb/U and Pb/Pb result in a measurement error of ~1-2% (at 2-sigma level) in the Pb/U age. The errors in measurement of Pb/Pb and Pb/Pb also result in ~1-2% (at 2-sigma level) uncertainty in age for grains that are >1.0 Ga, but are substantially larger for younger grains due to low intensity of the Pb signal. For most analyses, the cross-over in precision of Pb/U and Pb/Pb ages occurs at ~1.0 Ga.

^{204}Hg interference with ^{204}Pb is accounted for measurement of ^{202}Hg during laser ablation and subtraction of ^{204}Hg according to the natural $^{202}Hg/^{204}Hg$ of 4.35. This Hg is correction is not significant for most analyses because our Hg backgrounds are low (generally ~150 cps at mass 204).

Common Pb correction is accomplished by using the Hg-corrected Pb and assuming an initial Pb composition from Stacey and Kramers (1975). Uncertainties of 1.5 for Pb/Pb and 0.3 for Pb/Pb are applied to these compositional values based on the variation in Pb isotopic composition in modern crystal rocks.

Inter-element fractionation of Pb/U is generally ~5%, whereas apparent fractionation of Pb isotopes is generally <0.2%. In-run analysis of fragments of a large zircon crystal (generally every fifth measurement) with known age of 563.5 ± 3.2 Ma (2-sigma error) is used to correct for this fractionation. The uncertainty resulting from the calibration correction is generally 1-2% (2-sigma) for both Pb/Pb and Pb/U ages.

[1]Supplemental Information. Files S1–S2, Figures S1–S5, and Tables S1–S2. File S1 contains a detailed explanation of the methods used for detrital zircon data acquisition. File S2 contains a detailed explanation of the methods used for $^{40}Ar/^{39}Ar$ data acquisition and additional information on the sample presented in the text. Figures S1–S4 contain detailed measured sections of the Rainbow Gardens Formation from all four localities. Figure S5 contains individual probability plots for detrital zircon plots, as well as one for all Rainbow Gardens Formation samples combined. Tables S1 and S2 present raw detrital zircon data and calculations of maximum depositional ages, respectively. Please visit https://doi.org/10.1130/GES01127.S1 or the full-text article on www.gsapubs.org to view the Supplemental Information.

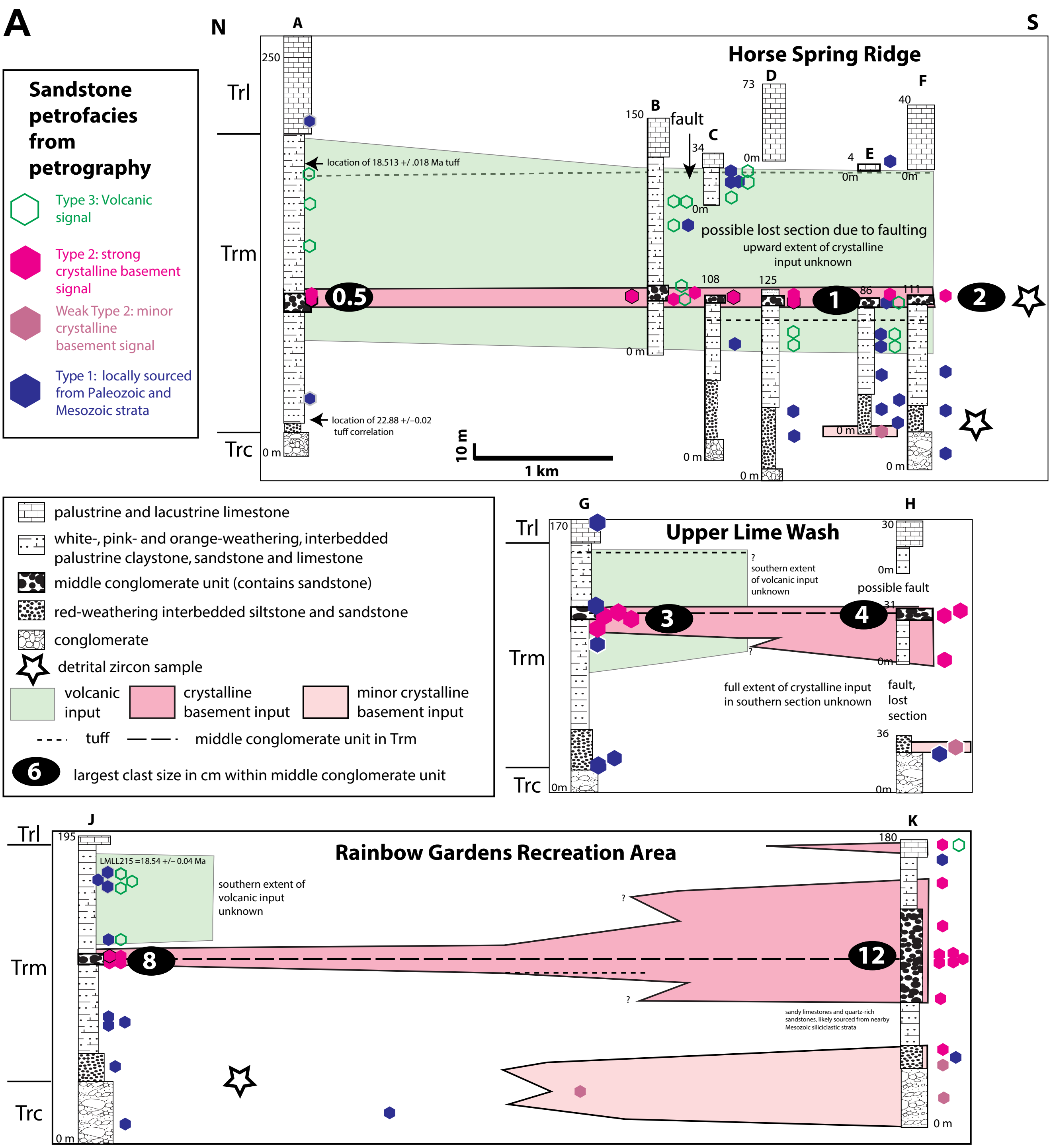

Figure 5 (*on this and following two pages*). Simplified stratigraphic columns with provenance and geochronology data. Measured sections have been simplified and show predominant lithologies or lithofacies associations. Distance between columns is shown to scale. Note vertical exaggeration. Section K overall thickness was determined by both field work and mapwork and is therefore slightly approximated. Trl—Rainbow Gardens Formation upper limestone unit; Trm—Rainbow Gardens Formation middle unit; Trc—Rainbow Gardens Formation basal conglomerate. (A) Simplified stratigraphy from the three north-south transects in the southern Rainbow Gardens Formation basin, with the locations of detrital zircon and sandstone samples by height in each section. Sandstone samples were assigned a petrofacies designation based on point counting and petrographic examination (see text for more details). Samples that plot on the diagram but not next to a column were collected in between measured sections, and their horizontal and vertical position relative to the other sections is shown. Background patterns show the occurrences of the volcanic and crystalline basement provenance signals.

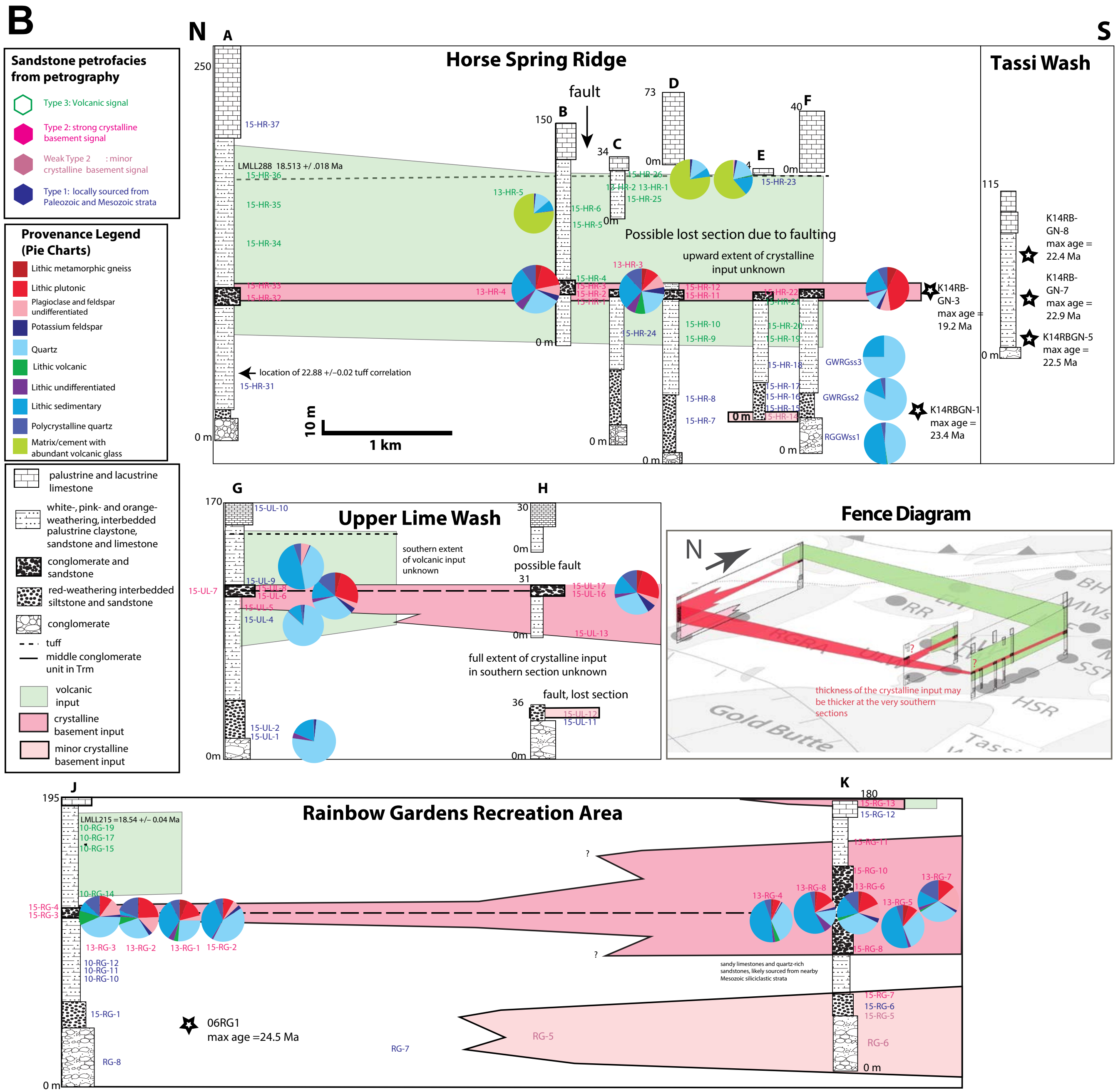

Figure 5 (*continued*). (B) Same diagram as A but with sample numbers and dates plotted along with detrital zircon maximum ages and point count results (pie charts). Reported maximum possible age of deposition for detrital zircon samples is based on the youngest single grain (YSG) method (see text for more details). Pie charts for RG-5 through RG-8 are from the basal conglomerate (Trc) shown on Figure 6. Additional stratigraphic column from Tassi Wash is shown but is not to horizontal scale. The Tassi Wash location is ~15 km south-southeast of the Horse Spring Ridge localities in the reconstruction on Figure 4. No sandstone samples are available from Tassi Wash (the road to Tassi Wash was removed by a flash flood, preventing a follow-up field season to this site). Fence diagram shows stratigraphic columns with petrofacies plotted on part of the Figure 4 base map: Note that the Proterozoic crystalline signal to the east may be thicker than shown due to possible lost section from faulting in the southernmost portion of the basin, i.e., the signal may persist upwards from the 19 Ma pulse.

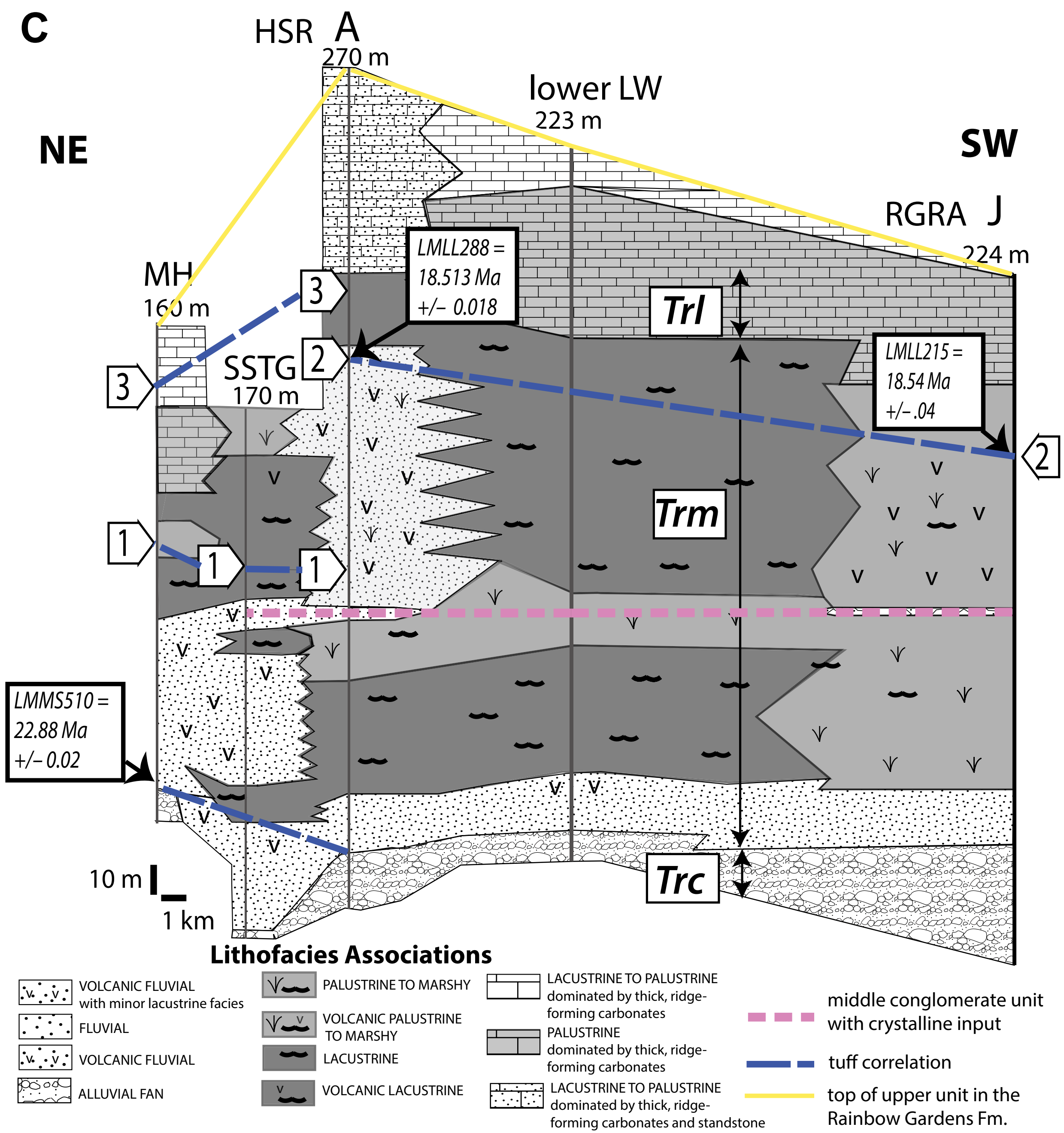

Figure 5 (*continued*). (C) Simplified stratigraphic sections on a cross section from northeast to southwest, modified from Lamb et al. (2015). See Figure 4 for location of transect. Note this includes two sections, A and J, shown in parts B and C here, in addition to new sections at Mud Hills (MH), south St. Thomas Gap (STTG), and lower Lime Wash (LW). Palustrine facies include a mix of carbonate, mudstone, and sandstone. Lacustrine facies are predominantly carbonate and mudstone. HSR—Horse Spring Ridge; RGRA—Rainbow Gardens Recreation Area; Trl—Rainbow Gardens Formation upper limestone unit; Trm—Rainbow Gardens Formation middle unit; Trc—Rainbow Gardens Formation basal conglomerate.

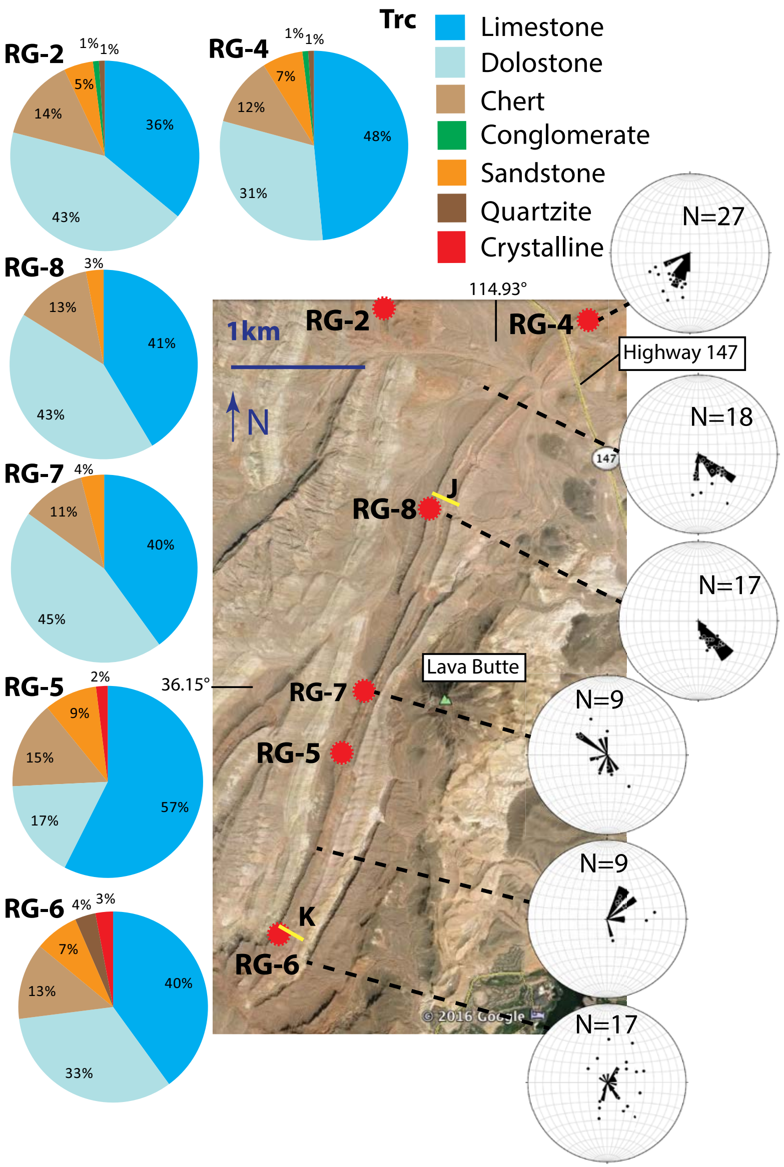

Figure 6. Provenance and paleocurrent data from the Rainbow Gardens Formation basal conglomerate (Trc) at the Rainbow Gardens Recreation Area, just east of Las Vegas, with sample locations shown on a Google Earth image. See Figure 4 for location. Pie charts show conglomerate clast count results of Rice (1987). Crystalline rocks include metamorphic and plutonic grains. Stereonet data show paleocurrent direction based on imbricated clasts within the basal conglomerate (Trc). Stereonets were plotted using the Stereonet program of Allmendinger et al. (2012).

transects of measured sections from three well-exposed ridges as well as a single measured section from Tassi Wash. The lithology of the measured sections in Figure 5 has been greatly simplified (original detailed measured sections are shown in Figures S1–S4 [footnote 1]). We correlated sections using a distinctive pebbly conglomerate unit in the middle of the sections, tuffs presented in Lamb et al. (2015), and a newly found tuff that we traced laterally between sections at Horse Spring Ridge and Upper Lime Wash, which occurs ~2.5 m below a tuff dated at 18.513 ± 0.018 Ma (gray dotted line on Figs. 5A and 5B).

The base of the sections from the southern basin contains a conglomeratic unit interpreted as fluvial deposits on alluvial fans (Fig. 3; Trc of Lamb et al., 2015). Figure 6 shows paleocurrent data from the Rainbow Gardens Recreation Area location. Data from the conglomerate show multiple flow directions, consistent with the interpretation of Lamb et al. (2015) that these deposits formed on alluvial fans, or bajadas, sourced from the south, north, and east. The conglomerate is overlain by the middle Rainbow Gardens Formation unit (Trm), which typically contains a predictable sequence of strata. The lowest is a red-weathering, interbedded sandstone and siltstone facies that represents deposition within a finer-grained (compared to the underlying conglomerate) fluvial system. This is overlain by a white-weathering, mixed sequence of sandstone, mudstone, limestone, and dolostone that documents palustrine to lacustrine conditions. The middle of every section in the southern part of the basin contains a distinctive conglomerate bed or sequence of coarser clastic beds (called the middle conglomerate unit hereafter), representing increased energy in a fluvial system (Figs. 5A and 5B). This is followed by a return to palustrine and lacustrine conditions with local fluvial input. The middle Rainbow Gardens Formation unit is capped by a limestone unit (Trl of Lamb et al., 2015) that records a low-gradient landscape in which lacustrine to marshy environments developed across the basin.

Although every section contains this same general vertical sequence of facies, there are notable differences in the thicknesses and clast sizes of the middle conglomerate unit, as well as lateral facies changes in the upper part of the middle unit. The basal and middle conglomerate units at the Rainbow Gardens Recreation Area section (Fig. 5A) are thickest and contain the largest clasts. Within each north to south transect, the middle conglomerate unit thins to the north and contains progressively smaller clasts (Figs. 5A and 5B). The middle conglomerate unit also fines from the Rainbow Gardens Recreation Area eastward toward Horse Spring Ridge, but we cannot determine its total thickness at sections C–F and H until additional mapping is completed. We note that there is not a comparable coarse pulse of sedimentation at other margins around the basin (Lamb et al., 2015); instead, there is fairly steady deposition of volcaniclastic sandstones sourced from the north throughout much of the middle unit (Trm) across the basin.

We also note that the overall thickness of the upper part of the middle unit (Trm) from the middle conglomerate unit to the base of the upper limestone (Trl) at section A at the Horse Spring Ridge locality is thicker than other sections, including section J at Rainbow Gardens Recreation Area and the Mud Hills section (Fig. 5C). Schmidt (2014) documented a similar thickening in the upper part of the middle unit, from Mud Hills southward to the South St. Thomas Gap sections (for additional details, see Schmidt, 2014). Prior to the deposition of the middle conglomerate unit, the thickness of the middle unit (Trm) is uniform across the basin (for additional details, see Lamb et al., 2015), but above the middle conglomerate, section A thickens relative to surrounding locations.

To the southwest, roughly coeval conglomerate facies that are not part of the Rainbow Gardens Formation are found east of the Spring Mountains near Sloan and Jean, Nevada, and within the McCullough Mountains and Lucy Gray Range between Jean and Nelson (Fig. 1). Near the town of Jean, these outcrops, (Jean Conglomerate of Hanson, 2008; also called Tertiary Roundstone gravels by Garside et al., 2012) rest on the Permian Hermit Formation, are overlain by the 15.2 Ma Tuff of Bridge Spring, and contain mainly Paleozoic carbonate clasts (Garside et al., 2012, and references therein). Northeast of these and southwest of Sloan, similar deposits, called “Tertiary fluvial gravels” by Hinz et al. (2015), rest on the Pennsylvanian–Permian Bird Spring Formation but contain crystalline basement clasts in addition to Paleozoic carbonate clasts. The McCullough Springs conglomerate in the central McCullough Mountains, southeast of Jean, was thought to be deposited sometime between 40 and 23 Ma (Herrington, 1993), but it is no younger than the overlying 18.78 ± 0.02 Ma Peach Spring Tuff (Ferguson et al., 2013). Most localities of the McCullough Springs conglomerate contain 50%–100% Proterozoic crystalline basement clasts, with additional Paleozoic sedimentary clasts. Herrington (1993) speculated that the conglomerate was (1) deposited in roughly east-west paleochannels with easterly flow directions, and (2) sourced locally first and then from the thrust terrane to the west.

Similar-age deposits to the southeast of the Rainbow Gardens Formation include the Buck and Doe Conglomerate (Young and Crow, 2014), a locally derived gravel sequence on the Hualapai Plateau south of the Grand Canyon that overlies the Paleocene–Eocene Music Mountain Formation and contains a tuff dated at 24.12 ± 0.04 Ma ($^{40}Ar/^{39}Ar$ from Young and Crow, 2014) near the top of the sequence. Its lower member is dominated by Cambrian through Mississippian carbonate clasts that were eroded from local cliffs and mesas, whereas the upper, arkosic member contains Proterozoic basement clasts, including distinctive types that identify the source area as local exposures in the southern Hualapai Plateau (Young and Crow, 2014). The Buck and Doe Conglomerate covered the Hualapai Plateau and formed a fairly uniform surface across which early Miocene volcanic flows were deposited (e.g., Young and Hartman, 2014).

Conglomerate and Sandstone Provenance Data

Provenance data (Figs. 5–7; Table 1) document the compositional range of the clastic units. We identified three distinct petrofacies. Type 1 petrofacies (Fig. 7A) contains quartz, calcite, limestone, chert, and lithic sedimentary grains and was derived from the nearby Paleozoic passive margin and Mesozoic nonmarine strata. Type 2 (Fig. 7B) has many of the same grains as type 1 but with a significant addition of plutonic and metamorphic grains, mainly gneiss. Type 3 (Fig. 7C) has type 1 or 2 grains mixed with a volcanic component, including glass shards, lithic volcanic clasts, volcanic quartz grains, and tuffaceous material.

Within the basal conglomeratic unit of the Rainbow Gardens Formation, the crystalline basement clasts and grains of type 2 only show up in the southern Rainbow Gardens Recreation Area transect (Figs. 5A and 6). Rice (1987) presented clast counts for the basal Rainbow Gardens Formation conglomerate throughout the Rainbow Gardens Recreation Area locality. His two southernmost sample locations (RG-5 and RG-6) match our type 2 petrofacies, sourced predominantly from local Paleozoic limestone and Mesozoic siliciclastic formations, but with up to 3% of crystalline basement input, namely, granite and gneiss. His other sections to the north, including ones north of the Rainbow Gardens Recreation Area transect (Fig. 5), are type 1 sandstones (Rice, 1987; see also Fig. 6). Beard (1996) similarly noted a predominance of Paleozoic limestone lithologies with additional Mesozoic siliciclastic clasts in the basal conglomerate at Horse Spring Ridge and Upper Lime Wash localities (Fig. 4). These eastern locations were further examined as part of this study, and no crystalline basement clasts were observed. The basal conglomerate units at these two localities contain only type 1 petrofacies.

Sandstones and conglomerates in the middle unit of the Rainbow Gardens Formation record variations of the three petrofacies types (Fig. 5). All locations have type 1 petrofacies sandstones. The Rainbow Gardens Recreation Area transect contains the greatest vertical and lateral extent of type 2 petrofacies, i.e., the greatest overall input of a crystalline basement signal (Fig. 5). At Rainbow Gardens Recreation Area, the Proterozoic signal is present in sandstone and conglomerate beds throughout much of the middle unit (Fig. 5). Eastward, the crystalline basement signal shows up clearly within the middle conglomerate, with a slight hint of the signal lower in the middle unit, just above the basal conglomerate, but this is based on only 1–2 grains (Fig. 5). These eastern transects show less of the crystalline basement signal as the middle conglomerate unit thins from west to east. At the Upper Lime Wash and Rainbow Gardens Recreation Area locations, the crystalline basement–bearing middle conglomerate unit also thins from south to north. At the Horse Spring Ridge locality, the type 2 crystalline basement signal is found in a 1–3m-thick middle clastic unit that contains a few pebble-granule–bearing sandstones. Thus, the type 2 signal is greatest in the southwest and least in the northeast.

The type 3 petrofacies records volcanic input in a pattern opposite that of petrofacies type 2: The signal is strongest in the north and east sections and nonexistent in the southwest. The northernmost measured section A at Horse Spring Ridge has volcaniclastic sandstones, reworked tuffs, and tuffs throughout much of the measured section. This signal extends to the southern Horse Spring Ridge sections as well. The signal is also present at the northern end of the Rainbow Gardens Recreation Area and Upper Lime Wash. In the southern parts of the basin, the type 3 volcanic signal is present only present in the middle and upper parts of the middle unit (Fig. 5A), but Figure 5C and data

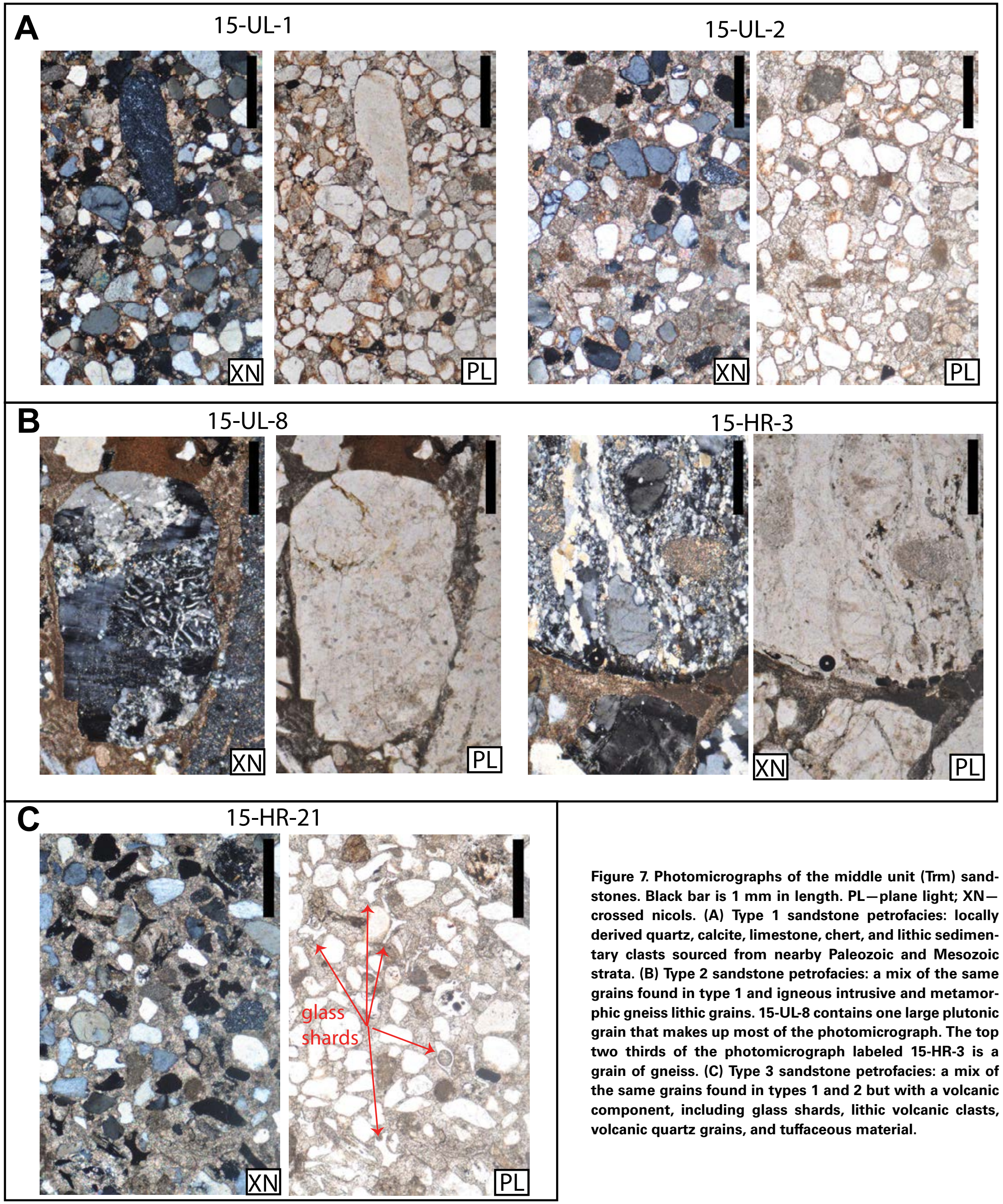

Figure 7. Photomicrographs of the middle unit (Trm) sandstones. Black bar is 1 mm in length. PL—plane light; XN—crossed nicols. (A) Type 1 sandstone petrofacies: locally derived quartz, calcite, limestone, chert, and lithic sedimentary clasts sourced from nearby Paleozoic and Mesozoic strata. (B) Type 2 sandstone petrofacies: a mix of the same grains found in type 1 and igneous intrusive and metamorphic gneiss lithic grains. 15-UL-8 contains one large plutonic grain that makes up most of the photomicrograph. The top two thirds of the photomicrograph labeled 15-HR-3 is a grain of gneiss. (C) Type 3 sandstone petrofacies: a mix of the same grains found in types 1 and 2 but with a volcanic component, including glass shards, lithic volcanic clasts, volcanic quartz grains, and tuffaceous material.

TABLE 1. POINT COUNT DATA FROM SANDSTONES

Raw Data																			
					Plagioclase and feldspar undifferentiated		Lithic sedimentary						Polycrystalline quartz						
Sample	Latitude*	Longitude*	Quartz	Potassium feldspar	Plagioclase feldspar	Feldspar undifferentiated	Lithic sedimentary (Ls)	Limestone	Calcite	Lithic volcanic (Lv)	Lithic plutonic (Lp)	Lithic metamorphic gneiss (Lmg)	Lithic metamorphic polycrystalline quartz (Lmqp)	Microcrystalline quartz (lithic)	Polycrystalline quartz	Lithic und. (Lu)	Matrix/cement	Hornblende	**Total**
13-HR-1†	36.31268	–114.145901	54	4	6		38	7		3				2	1	1	184		300
13-HR-2†	36.313236	–114.145608	41		6		17	4									232		300
13-HR-3	36.313334	–114.145959	44	20	7	4	22	18		16	20	8	15	14	14	15	83		300
13-HR-4	36.317375	–114.146769	55	16	4	4	27	16	1	1	38	9	13	9	9	13	85		300
13-HR-5†	36.31706	–114.146166	37	1	4		6	9	7					3	2		231		300
RGGW SS1§	36.3006	–114.1576	77		1		79			1					5		137		300
RGGW SS2§	36.3007	–114.1574	146				26								7		121		300
RGGW SS3§	36.3008	–114.1568	122				2	4	31					4			138		300
RGGW SS4§	36.0094	–114.1562	23	16		6	10	32			84	15	4		12	5	129		336
13-RG-1	36.17075	–114.936986	46	7			21	33	3	6	26	11	10	2	3	8	124		300
13-RG-2	36.17075	–114.936986	56	27	3	3	6	1		13	46	2	22		15	3	103		300
13-RG-3	36.17075	–114.936986	68	21	3		9	3		18	16		11		9		142		300
13-RG-4	36.119592	–114.960413	39	1	1		29	14	4	4	6	2	4	5	2	2	187		300
13-RG-5	36.119592	–114.960413	43	2			15	38	8		10	6	3	7	4	3	161		300
13-RG-6	36.119592	–114.960413	76	23	4	3	14	16	4	5	32	6	12	2	12		91		300
13-RG-7	36.119592	–114.960413	50	30		3	8	9		2	21		16	3	11	4	65		222
13-RG-8	36.119592	–114.960413	28	10	4		14	75			29	4	4	23	4	13	92		300
15-RG-2	36.169425	–114.9361777	53	2	0	0	2	13	26	0	12	16	0	9	1	0	166	0	300
15-UL-1	36.302974	–114.2330542	133	0	1	2	2	8	15	0	0	0	0	7	1	7	124	0	300
15-UL-4	36.302628	–114.2344804	155	0	2	0	3	5	10	0	0	0	0	1	4	1	119	0	300
15-UL-8	36.302667	–114.2318514	53	6	3	3	13	6	1	0	41	7	0	1	22	4	64	0	224
15-UL-9	36.302666	–114.2318514	53	8	1	0	4	30	22	0	0	0	0	6	7	0	169	0	300
15-UL-16	36.280391	–114.2382265	60	11	1	12	17	7	1	0	51	9	2	4	22	2	98	2	299

*North American datum (NAD) 27 horizontal datum.
†Samples that have a matrix rich in glass shards.
§Approximate locations: Samples were collected prior to global positioning system (GPS) technology.

from Lamb et al. (2015) and Beard (1996) show its presence throughout the middle unit farther north in the basin. The volcanic signal is from both air-fall and fluvial processes: Pristine glass shards show little signs of reworking, whereas other sandstones contain volcanic grains that have been rounded by transport.

Discussion of Provenance Results

The crystalline basement signal in the type 2 rocks was likely derived from exposures of crystalline basement rocks to the south (Fig. 2; Rice, 1987). Figure 2 shows the extent of Proterozoic units exposed today south of Lake Mead, from the Lucy Gray and McCullough Ranges near I-15 south of Las Vegas to the White Hills south of Gold Butte. During the early Miocene, however, crystalline basement was likely widely exposed in this region: Many of the ca. 20–13 Ma volcanic deposits rest directly on basement. (We note, however, that some Proterozoic units, including ones exposed at Gold Butte and the White Hills, were not exposed prior to extension but were exhumed during extension [e.g., Fitzgerald et al., 1991, 2009].) It is also possible that some of the crystalline basement signal was recycled from Cenozoic conglomerate units flanking the Kingman Uplift, including the conglomerates in the Jean and Sloan quadrangles and the McCullough Springs Conglomerate. Herrington (1993) noted that the McCullough Spring Conglomerate rests on crystalline basement and varies in clast composition from 55% to 100% crystalline basement rock.

A fluvial influx of volcanic sediment into the Rainbow Gardens Formation basin from the north was first described by Beard (1996), and new dates on volcanic tuffs were reported in Lamb et al. (2015). The volcanic signal of type 3 sandstones is mainly derived from the Caliente volcanic field to the north (e.g., Best et al., 2013).

There is also evidence for a western sediment source beginning in the basal conglomerate of the Rainbow Gardens Formation. Rice (1987) found two distinct types of quartzite: highly indurated varieties in the far southern Rainbow Gardens Recreation Area sections, which he thought resembled Cambrian Tapeats Sandstone and Wood Canyon Formation, and clasts of white, well-sorted, fine- to medium-grained quartzite throughout the Rainbow Gardens Recreation Area that are likely Eureka Quartzite. Eureka Quartzite clasts are also found in the southern Lime Wash area in the Virgin Mountains but not anywhere farther north or east. The Eureka Quartzite is an Ordovician passive-margin unit that thins eastward. Isopachs of the Eureka Quartzite indicate the nearest sources for clasts of the unit are in thrust plates west of the Keystone thrust in the Spring Mountains (Fleck, 1970), and in the upper plate of the Dry Lake thrust in the Dry Lake Range west of the Muddy Mountains (Beard et al., 2007). This provenance interpretation supports evidence from paleocurrent data (Fig. 6) at the Rainbow Gardens Recreation Area that record a component of easterly flow.

Detrital Zircon Results

We present detrital zircon data from six Rainbow Gardens Formation samples collected at three locations (Figs. 4, 5, and 8; see also Fig. S5; Tables S1 and S2 [footnote 1]). These samples were collected specifically to address whether the detrital zircon signature would reveal a component of eastern Colorado Plateau sediment consistent with input from an ancestral Colorado River. In addition to the Rainbow Gardens Formation samples, we present three detrital zircon samples from Oligocene–early Miocene conglomeratic units described above and two samples from the Cretaceous Lavinia Wash Formation (Figs. 1, 2, 4, and 8; see also Fig. S5; Table S1 [footnote 1]). Two samples of arkosic Buck and Doe Conglomerate were collected along the Grand Wash Cliffs: B14–088 was collected just south of the mouth of the Grand Canyon in a conglomeratic sandstone underlying an 18.00 ± 0.02 Ma basalt at Iron Mountain (File S2 [footnote 1]), and B14_085 is from a sandstone below ca. 20 Ma basalts and the Peach Springs Tuff (Young and Brennan, 1974) just north of Hackberry, Arizona (Fig. 2). Detrital zircon sample 06JE1 (Figs. 2 and 8; Hanson, 2008) is from the Jean Conglomerate north of Jean, Nevada, which underlies the 15.4 Ma Tuff of Bridge Spring. Figure 9 presents two samples of the ca. 100 Ma Lavinia Wash Formation, located west of Sloan (Nevada) in the Spring Mountains (Figs. 1, 2, and 9; Hanson, 2008).

First, we used the Kolmorogov-Smirnoff (K-S) test to compare sample populations and determine the samples, if any, that are not statistically distinguishable and therefore might have the same source areas (Figs. 8A, 9A, and 9B; following the methods of Dickinson and Gehrels, 2009). Gehrels et al. (2011) pointed out that the K-S statistic is very sensitive to the proportions of ages present, so that if two samples have somewhat different proportions of the same age groups, the samples could have a similar source even with low *P* values. Although most Rainbow Gardens Formation samples are weakly to moderately congruent, suggesting similar source areas, low *P* values in some comparisons indicate either local variability or that the sample size (n = ~100 grains) was too small (Fig. 8). A strongly congruent relationship (*P* = 0.98) between RBGN3 from the middle conglomerate unit at Horse Spring Ridge and RBGN7, the middle sandstone at Tassi Wash, and the cumulative and stacked probability plots (Figs. 8B and 8C) indicate these sandstones have a very similar detrital zircon signature and likely the same source area. Although the Tassi Wash section does not contain pebbly sandstone beds, the strongly congruent *P* value of 0.98 (Fig. 8A) suggests the clastic sequence sampled at Tassi Wash is the distal equivalent of the middle conglomerate unit. We do not have point-count data from Tassi Wash to test this correlation.

The Jean Conglomerate and Buck and Doe Conglomerate samples show little statistical similarity with each other and especially with the Rainbow Gardens Formation, as indicated by *P* values of <0.05 (Fig. 8A). The Jean and Iron Mountain samples, shown as the blue and green lines on the cumulative probability plot (Fig. 8D), are weakly congruent (*P* = 0.08), probably because of the strong Yavapai-Mazatzal peaks in both samples (Figs. 8D and 8E). The Jean sample and the lowest sandstone at Tassi Wash (K14_RGBN-5) also share the weak Grenville and strong Yavapai-Mazatzal peak (Figs. 8C and 8E).

Lavinia Wash (ca. 100 Ma) detrital zircon data, when compared with a sample of the ca. 72 Ma quartzite-volcanic clast conglomerate of the Canaan Peak Formation (Fig. 1) in southwest Utah (Larsen et al., 2010), suggest they could have a similar source or that the Lavinia Wash was reworked into the Canaan Peak unit (Fig. 9). Both deposits contain clasts of ca. 100 Ma Delfonte volcanics (Goldstrand, 1992) and yield a *P* value of 0.84 when comparing grains older than ca. 150 Ma. Removing grains younger than 150 Ma (Figs. 9E and 9F) removes the effect of the overwhelming number of ca. 95–110 Ma zircons in the Lavinia Wash samples (Fig. 9C), but the results should be viewed as suggestive only, because the remaining number of grains for comparison is extremely small (*n* = 27).

Second, we examined stacked probability plots that show dominant peaks in zircon populations (Figs. 8C and 8E) to understand the possible source areas for the Oligocene–Miocene deposits. Rainbow Gardens Formation detrital zircon age distributions (Figs. 8B, 8C, and 8F) reflect several sources, including both primary-sourced and recycled Oligocene–Miocene volcanics (19–28 Ma), and recycled Mesozoic Cordilleran magmatic arc (ca. 280–70 Ma), Grenville sources (ca. 1250–850 Ma), 1.4 Ga anorogenic granite, and ca. 1.7–1.6 Mazatzal-Yavapai sources (e.g., Dickinson et al., 2012; Gehrels et al., 2011). Similarly, the Jean Conglomerate sample shares those same peaks (Figs. 8D and 8E; Fig. S5 [footnote 1]). The Buck and Doe Conglomerate samples (Fig. 8E; Fig. S5 [footnote 1]) display the Oligocene–Miocene, 1.4 Ga anorogenic granite and Mazatzal-Yavapai signals and a weak Cordilleran magmatic arc (164–90 Ma) signal.

A

K-S P-values using error in the CDF

		Garden Wash		Tassi Wash			RCRA		Buck and Doe Conglomerate	
		RBGN 1	RBGN 3	RGBN 5	RGBN 7	RGBN 8	06RG1	JeanCgl	Hackberry	Iron Mtn
RBGN 1	Garden Wash		**0.289**	0.023	**0.075**	0.020	**0.293**	0.000	0.000	0.000
RBGN 3		**0.289**		**0.262**	**0.982**	**0.398**	0.009	0.000	0.000	0.000
RGBN 5	Tassi Wash	0.023	**0.262**		**0.339**	0.003	0.001	0.001	0.000	0.000
RGBN 7		**0.075**	**0.982**	**0.339**		**0.227**	0.008	0.000	0.000	0.000
RGBN 8		0.020	**0.398**	0.003	**0.227**		0.000	0.000	0.000	0.000
06RG1	RCRA	**0.293**	0.009	0.001	0.008	0.000		0.000	0.000	0.000
Jean Conglomerate		0.000	0.000	0.001	0.000	0.000	0.000		0.000	**0.076**
Buck and Doe Conglomerate Hackberry		0.000	0.000	0.000	0.000	0.000	0.000	0.000		0.000
Buck and Doe Conglomerate Iron Mtn		0.000	0.000	0.000	0.000	0.000	0.000	**0.076**	0.000	

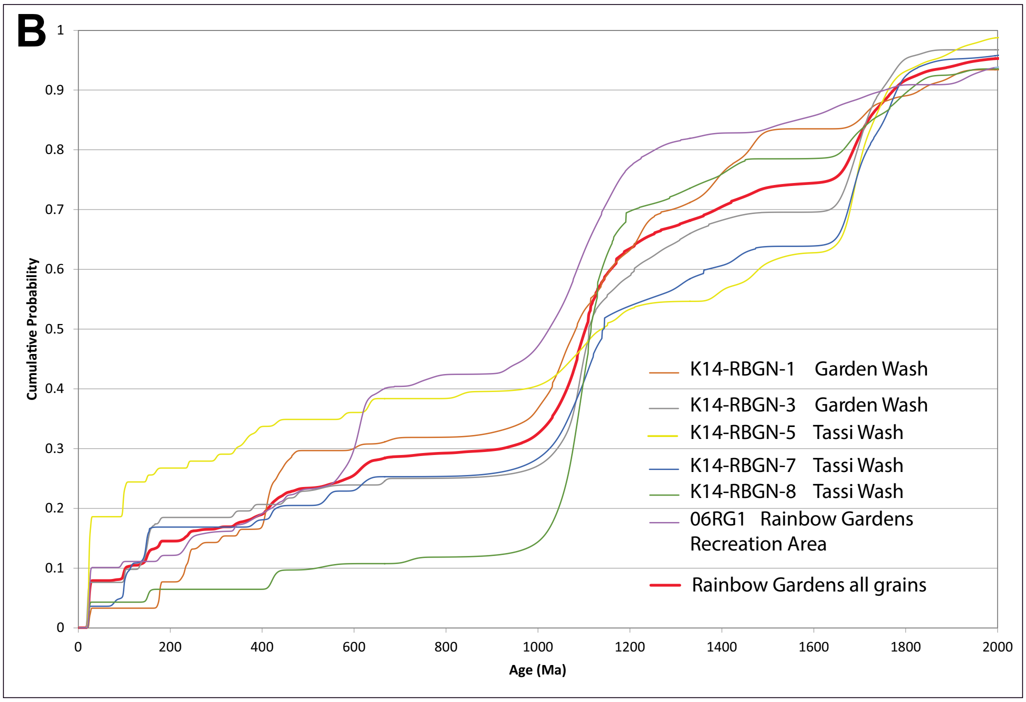

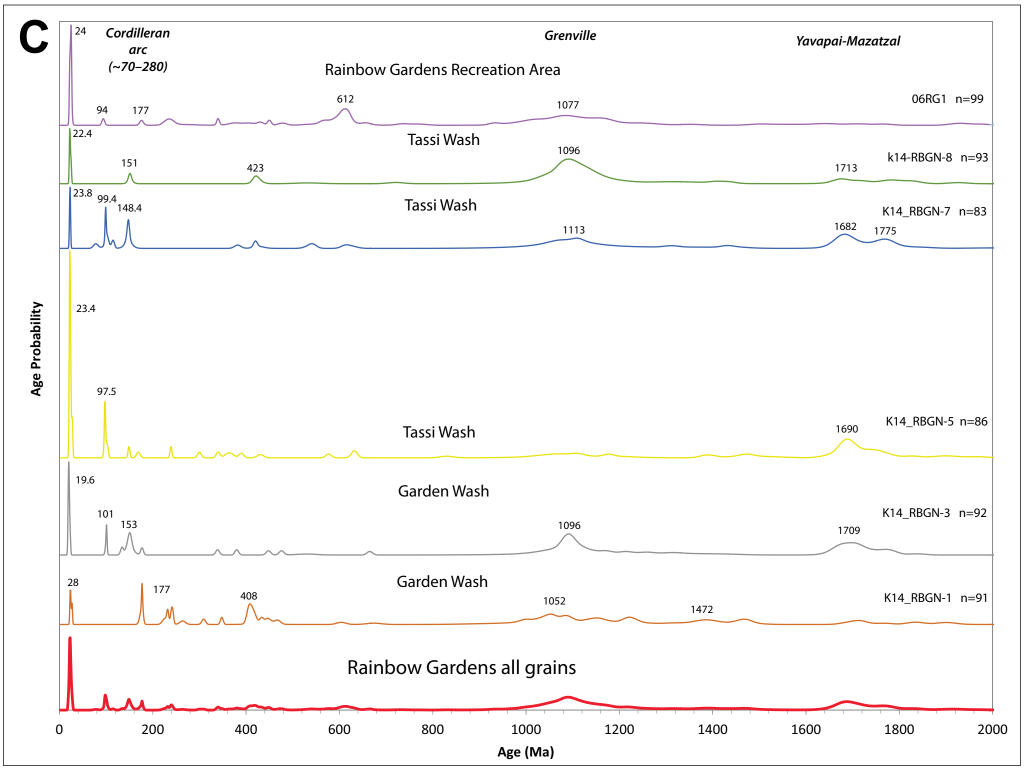

Figure 8 (***on this and following page***). **Detrital zircon data for all late Oligocene–early Miocene samples from the Rainbow Gardens Formation and the Jean and Buck and Doe Conglomerates. See Figure 5 for locations of samples within stratigraphic sections and Figures 2 and 4 for geographic locations. (A) Kolmogorov-Smirnov (K-S) statistics for all Oligocene–Miocene samples. CDF—cumulative distribution function; RCRA—Rainbow Gardens Recreation Area. (B) Cumulative probability plot for individual Rainbow Gardens Formation samples. (C) Stacked normalized probability plots for individual Rainbow Gardens Formation samples.**

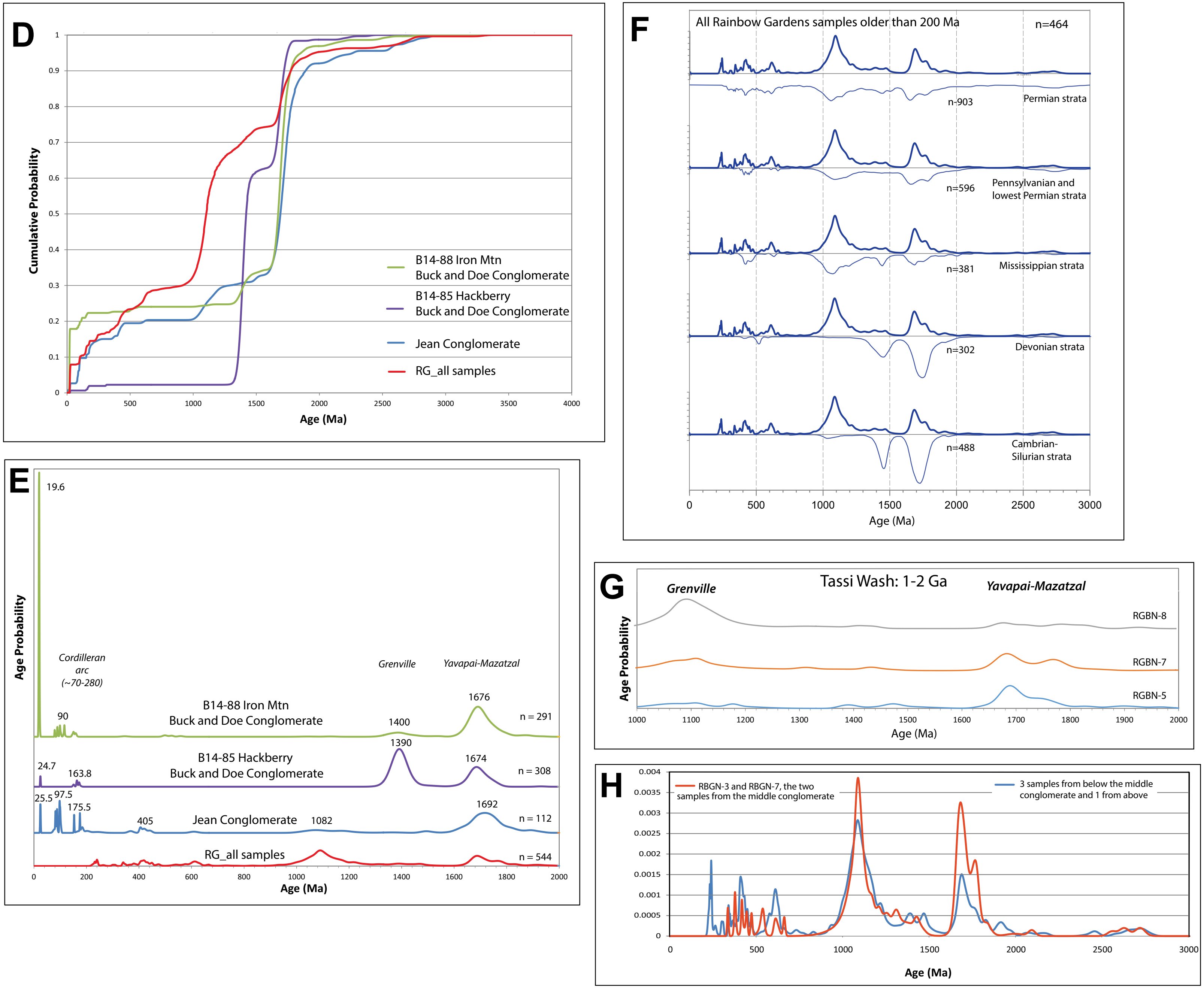

Figure 8 (*continued*). (D) Cumulative probability plot for all Rainbow Gardens (RG) Formation samples combined and for samples south of the paleoscarp of Permian strata, the Jean and Buck and Doe Conglomerates. (E) Stacked normalized probability plots for all Rainbow Gardens Formation samples combined and for samples south of the paleoscarp of Permian strata, the Jean and Buck and Doe Conglomerates. (F) Comparison of probability plots of the combined Rainbow Gardens Formation samples, shown by the upper bold blue lines, versus Paleozoic strata of the Grand Canyon, shown by the lower blue lines, from Gehrels et al. (2011). (G) Stacked normalized probability plot for the three Tassi Wash samples from 1 to 2 Ga. (H) Combined probability plots of the two samples from the Rainbow Gardens Formation middle conglomerate unit, shown in red, and the samples from above and below the middle conglomerate unit, shown in blue.

A

K-S P-values using error in the CDF	LW-1	LW-2	Canaan Peak
LW-1		0.000	0.000
LW-2	0.000		0.000
Canaan Peak_Larsen	0.000	0.000	

K-S P-values for no error	LW-1	LW-2	Canaan Peak
LW-1		0.000	0.000
LW-2	0.000		0.000
Canaan Peak_Larsen	0.000	0.000	

Average K-S P-values using Monte-Carlo	LW-1	LW-2	Canaan Peak
LW-1		0.000	0.000
LW-2	0.000		0.000
Canaan Peak_Larsen	0.000	0.000	

B

K-S P-values using error in the CDF	LW-1 and 2	Canaan Peak
LW-1 and 2		**0.839**
Canaan Peak_Larsen	**0.839**	

K-S P-values for no error	LW-1 and 2	Canaan Peak
LW-1 and 2		0.783
Canaan Peak_Larsen	0.783	

Average K-S P-values using Monte-Carlo	LW-1 and 2	Canaan Peak
LW-1 and 2		0.646
Canaan Peak_Larsen	0.646	

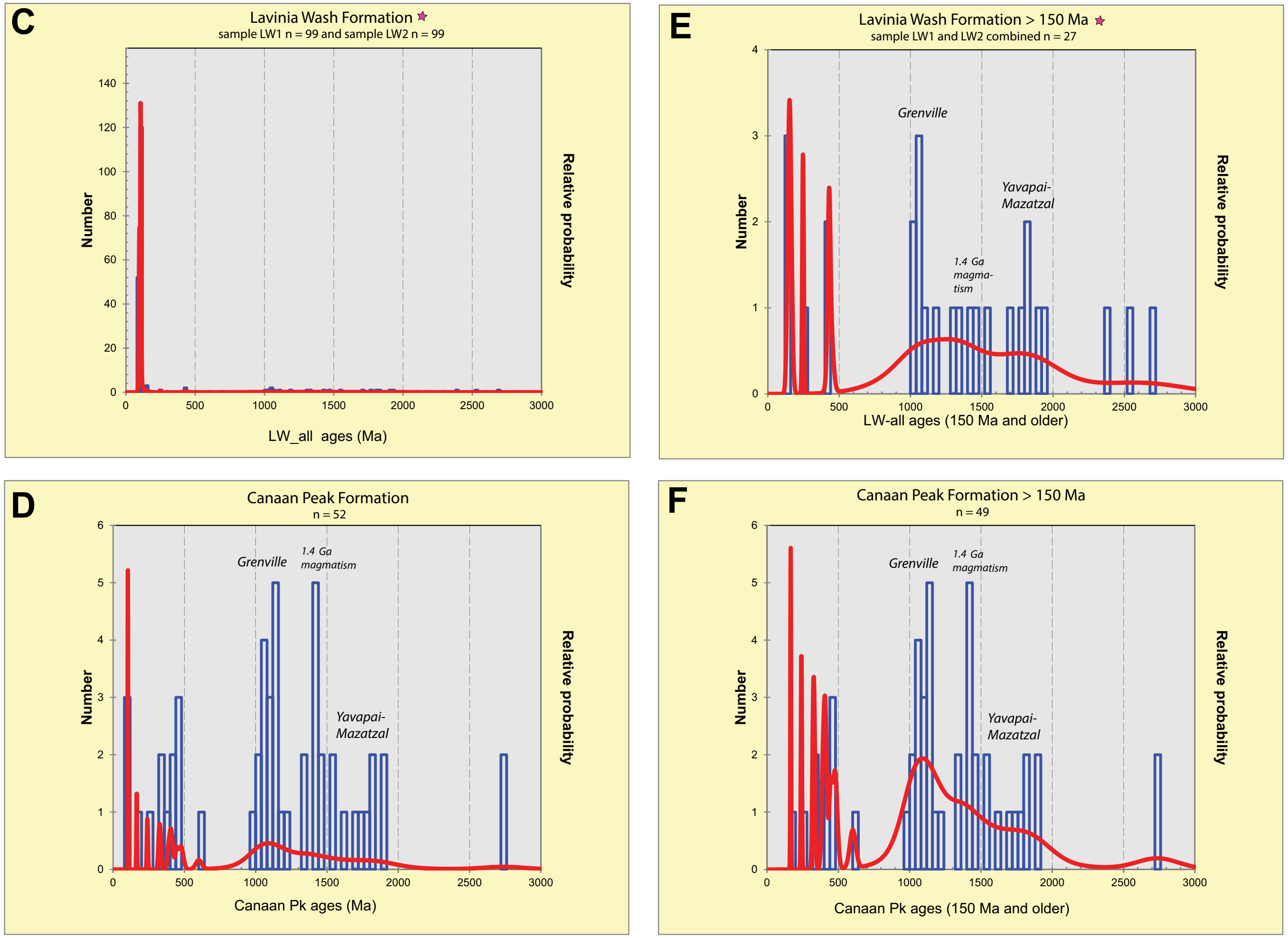

Figure 9. Comparison of detrital zircon data from the Cretaceous Lavinia Wash and Canaan Peak Formations. CDF—cumulative distribution function. (A) Kolmogorov-Smirnov (K-S) statistics and normalized probability plots for Lavinia Wash, samples LW1 and LW2 combined, and Canaan Peak. (B) Same as A but for grains older than 150 Ma. (C) Normalized probability plot for Lavinia Wash samples LW1 and LW2 combined. (D) Normalized probability plot for the Canaan Peak (Pk) Formation sample (Larsen et al., 2010). (E) Normalized probability plot for grains older than 150 Ma from the Lavinia Wash samples LW1 and LW2 combined. (F) Normalized probability plot for grains older than 150 Ma from the Canaan Peak Formation.

Discussion of Detrital Zircon Results

All Rainbow Gardens Formation samples have a 28–19 Ma signal (Figs. 8B and 8C) that likely reflects input from the Indian Peak and Caliente volcanic fields (36–18 Ma) to the north. We infer that the younger detrital zircons derive from air-fall processes. The ages bracket the younger part of the Indian Peak–Caliente field (18.51 Ma Hiko Tuff to 27.90–23.04 Ma Isom Formation; Best et al., 2013), as well as ca. 24–18 Ma tuff ages from the Rainbow Gardens Formation (Beard, 1996; Lamb et al., 2015). The peaks suggest much of the detrital zircon signal may be related to eruption of rhyolite ignimbrites in the southern part of the field after 24 Ma, as described by Best et al. (2013). The Hackberry Buck and Doe and Jean Conglomerate samples (Fig. 8E; Table S1 [footnote 1]) each have two grains of ca. 25–24 Ma age, and this suggests they are likely correlative in age to the Rainbow Gardens Formation basal conglomerate. The Iron Mountain Buck and Doe Conglomerate sample (Fig. 8E; Tables S1and S2 [footnote 1]) has a large number grain ages from 23 to 18.5 Ma and is equivalent in age to the middle unit of the Rainbow Gardens Formation. Oligocene–Miocene zircons in the Iron Mountain Buck and Doe and Jean Conglomerate samples may be sourced from either the north or south, whereas the Buck and Doe Hackberry location lies farther south, and it was likely sourced from the Aquarius Mountains (Young and Crow, 2014).

A weak but persistent component (1%–8%) of Cordilleran magmatic arc–age grains (ca. 280–70 Ma; Dickinson et al., 2012) occurs in all samples (Figs. 8C and 8E). The peaks cluster at around 175 Ma, 150 Ma, ca. 100 Ma, and ca. 80 Ma. The Cretaceous Willow Tank and Baseline Sandstones, which are locally preserved below the basal unconformity of the Rainbow Gardens Formation, at both the Rainbow Gardens Recreation Area and in the Virgin Mountains, are one possible source. There are no available detrital zircon data for these Cretaceous formations, but tuffs within the Willow Tank Formation have been dated at 94.4 and 98.4 Ma (K-Ar biotite; Fleck, 1970), 101.6 Ma and 99.9 Ma (sensitive high-resolution ion microprobe [SHRIMP] reverse geometry [RG] zircon U-Pb; Troyer et al., 2006), and 98.68 Ma at the base, and 98.56 Ma near the top (^{40}Ar/^{39}Ar, sanidine; Pape et al., 2011). In addition, Wells (2016) reported a maximum depositional age of 101.7 +0.4/–0.5 Ma for sandstone at the base of the Willow Tank Formation. Other possible sources include the Cretaceous Lavinia Wash Formation and the Cretaceous conglomerate of Brownstone Basin:

(1) The Cretaceous Lavinia Wash Formation. A detrital zircon sample from a volcaniclastic facies (Table S1 [footnote 1]; Hanson, 2008) is dominated by zircons with a mean age of 98 Ma and is interpreted as a zircon tuff age (Fig. 9). A second sample from a carbonate clast facies within the Lavinia Wash Formation has a detrital zircon age population at 107 Ma and is also interpreted as a zircon tuff age.

(2) The Cretaceous conglomerate of Brownstone Basin, found in the Spring Mountains west of Las Vegas (Fig. 2). Wells (2016) reported maximum depositional zircon ages of 102.8 +1.0/–1.2 Ma, 103.3 +1.0/–1.1 Ma, and 102.1 +1.7/–0.9 Ma.

We note that latest Cretaceous plutons (ca. 72–68 Ma) were exposed at the surface locally prior to eruption of early, pre-extension (ca. 20 Ma) volcanic rocks in the core of the Kingman Uplift south of Lake Mead (Faulds et al., 2001). However, no zircons of that age are found in any of the deposits, which we infer is because any exposures were too small to be captured by our detrital zircon samples (n = ~100) and because the paleoscarp of Permian strata, discussed in more detail below, was a significant barrier to northward dispersal during Rainbow Gardens Formation time.

The lowest sandstone samples from all three Rainbow Gardens Formation locations and the Jean Conglomerate (Figs. 8C and 8E; Table S1 [footnote 1]) contain one to five zircons of Triassic age that were likely recycled from underlying or nearby exposures of the Lower Triassic Moenkopi and Middle Triassic Chinle Formations (Dickinson and Gehrels, 2008).

Finally, the Rainbow Gardens Formation samples (Figs. 8B, 8C, and 8F) show strong Grenville peaks (ca. 1 Ga), which are typical of rocks sourced from Upper Paleozoic Grand Canyon strata (Gehrels et al., 2011), and variable strength Yavapai-Mazatzal–age peaks. The exception is RBGN-5, the basal sample at Tassi Wash, which has a weak Grenville peak and strong Yavapai-Mazatzal signal, which may indicate a Lower Paleozoic and Proterozoic basement source (Figs. 8B and 8F). Upward in the section at Tassi Wash, the proportion of Grenville-age grains increases, while Yavapai-Mazatzal–age grains decreases (Fig. 8G); this likely reflects variable input from nearby Paleozoic sources. The two Rainbow Gardens Formation samples from the middle conglomerate unit, RBGN-3 and RBGN-7, show an increase in the Yavapai-Mazatzal peaks when compared to the other Rainbow Gardens Formation samples, and we suggest this reflects the addition of the crystalline basement signal (Fig. 8H). As mentioned above, the Jean and Iron Mountain Buck and Doe Conglomerate samples share strong Yavapai-Mazatzal peaks, whereas the Hackberry Buck and Doe Conglomerate sample has strong ca. 1.4 Ga and Yavapai-Mazatzal peaks (Fig. 8E), all likely sourced from exposures of Proterozoic crystalline basement rock in the eroded terrane of the Kingman Uplift. Both Buck and Doe Conglomerate samples have strong 1.4 Ga peaks compared to the Jean Conglomerate sample, and this likely reflects their relative positions on either side of the Kingman Uplift. Almeida (2014) reported new ages of ca. 1682 Ma for the Davis Dam, Lucy Gray, and Newberry Mountains plutons in SE Nevada, which were previously thought to be ca. 1.4 Ga. These plutons may be the source for some of the ca. 1670–1690 Yavapai-Mazatzal peaks in the detrital zircon plots.

In summary, the Rainbow Gardens Formation detrital zircon signature is best explained by a mixture of local volcanic input and the recycling of nearby strata, namely, Paleozoic and Mesozoic strata. Of these, the Upper Paleozoic Grand Canyon source seems to be the largest, based on comparisons with probability plots of Gehrels and Dickinson (2011) and Figure 8F. The probability plots from the middle conglomerate unit (with the crystalline basement signal) also indicate a dominant Upper Paleozoic source, but with an enhanced Yavapai-Mazatzal source (Fig. 8H). Finally, we suggest that the few Cordilleran magmatic arc grains are likely recycled from Cretaceous deposits that were once more widespread across the Lake Mead region.

Age Constraints and Sedimentation Rates

Three recent $^{40}Ar/^{39}Ar$ dates (shown in stratigraphic position on Figs. 3, 5A, and 5C; Lamb et al., 2015) and the detrital zircon data help to constrain the age of deposition of the southern part of the Rainbow Gardens Formation basin. The oldest $^{40}Ar/^{39}Ar$ date, 22.88 Ma ± 0.02 Ma, is from a location just north of the Horse Spring Ridge transect but correlates to ~21 m on the Horse Spring Ridge measured section A, based on observed stratigraphic details and new detrital zircon work (Daniel Conrad, 2017, personal commun.; Figs. 5A and 5C). A younger date, 18.51 ± 0.02 Ma, is from a tuff high in the Horse Spring Ridge section, at 180 m on section A (Figs. 5A and 5C). At the Rainbow Gardens Recreation Area section J, a similar-aged tuff, 18.54 Ma ± 0.04 Ma, is found at 173 m (Figs. 5A and 5C). These tuffs are most likely from the Caliente caldera. The 22.88 Ma ± 0.02 tuff may be equivalent to the 23.04 Ma Bauers Tuff and/or 22.56 Ma Harmony Hills tuff from the Caliente caldera (Best et al., 2013). The 18.51 ± 0.02 Ma tuff at Horse Spring Ridge is essentially identical to the Hiko Tuff at 18.51 Ma (Best et al., 2013), which is the youngest tuff from the Caliente volcanic field. Note that this is younger than the Peach Springs Tuff to the south, which has an age of 18.78 Ma (Ferguson et al., 2013). The ca. 18.5 Ma tuffs are near the top of the Trm unit and the base of the Trl unit.

We used calculated maximum depositional ages from detrital zircon data (Table S2 [footnote 1]) to estimate sedimentation rates. The maximum depositional ages of 19.2 Ma (YSG and YC1σ), 19.6 Ma (YPP), and 20.0 Ma (YC2σ) for the middle conglomerate unit at Garden Wash are congruent with $^{40}Ar/^{39}Ar$ tuff ages for the Rainbow Gardens Formation. Lamb et al. (2015) calculated a sedimentation rate of 32 m/m.y. at the Horse Spring Ridge locality for the entire middle unit of the Rainbow Gardens Formation. With the new detrital zircon data, we can now estimate a rate for the upper and lower parts of the middle unit (Table 2). If we use the 19.2 Ma YSG and YC1σ detrital zircon maximum depositional age of the middle conglomeratic unit at section F (K14-RBGN 3; Table S2 [footnote 1]) and apply it to the same stratigraphic interval at section A, where the middle conglomeratic unit is 80 m below the dated ca. 18.5 Ma tuff, this yields a minimum sedimentation rate of ~116 m/m.y. for the upper part of the middle unit. If we use the YPP maximum depositional age of 19.6 Ma for the middle conglomerate unit, then we get a rate of 73 m/m.y. Both of these rates are higher than the rates of 21 and 24 m/m.y. for the lower part of the middle unit (Table 2). We did not use the YC2σ age to calculate a sedimentation rate because this method was determined to typically produce an age older than the depositional age of the strata (Dickinson and Gehrels, 2009).

DISCUSSION

Sediment Sources and Pathways

Stratigraphic, petrographic, and detrital zircon data all indicate that the source for much of the Rainbow Gardens Formation sediment was from nearby and/or underlying Paleozoic to Lower Mesozoic strata. The southern Rainbow Gardens Formation was deposited on the north-sloping Kingman Uplift, which made up the southern margin of the basin (Lamb et al., 2015), and thus the

TABLE 2. SEDIMENTATION RATES OF THE MIDDLE UNIT AT HORSE SPRING RIDGE LOCATION, SECTION A

Bed	Height of bed in section (m)	Age/maximum depositional age (Ma)	Total distance between two beds (m)	Total time between two beds (m.y.)	Calculated sedimentation rate (m/m.y.)
Dated tuff with $^{40}Ar/^{39}Ar$ age	180	18.51			
Upper part of middle unit			80	0.69	116
Middle conglomerate unit with detrital zircon YSG/YC1σ maximum depositional age	100	19.2			
Lower part of middle unit			79	3.68	21
Correlation of tuff layer from Mud Hills to tuff LMLL 275 at Horse Spring Ridge section A	21	22.88			
Dated tuff with $^{40}Ar/^{39}Ar$ age	180	18.51			
Upper part of middle unit			80	1.09	73
Middle conglomerate unit with detrital zircon YPP maximum depositional age	100	19.6			
Lower part of middle unit			79	3.28	24
Correlation of tuff layer from Mud Hills to tuff LMLL 275 at Horse Spring Ridge section A	21	22.88			

Note: YSG—youngest single grain; YC1σ—youngest 1σ grain cluster; YPP—youngest from probability plot.

Permian and Triassic strata on the Kingman Uplift are likely a significant source of the Upper Paleozoic detrital zircon signature discussed above. Our new data further support the hypothesis of a northern to northeastern source of volcanic tuffs and detritus (Fig. 5), as previously suggested by Beard (1996) and Lamb et al. (2015). Most importantly, however, our data imply a new, previously unrecognized Proterozoic source from the southwest and allow for refinement of paleogeographic reconstructions for the southern portion of the basin and the geologic evolution of the region.

The abrupt input of crystalline basement sediment into the southwest part of the basin and the thinning and fining to both the east and north support a southwest source for the crystalline basement type 2 petrofacies. In the southernmost Rainbow Gardens Recreation Area, paleocurrent data combined with type 2 petrofacies in the basal conglomerate and lower middle unit (section K in Fig. 5) suggest that, from the start of Rainbow Gardens Formation deposition, the southwesternmost part of the basin received a small amount of sediment from Proterozoic crystalline basement ("x" on Fig. 10). The maximum pulse of the Proterozoic-source signal is marked by deposition of the crystalline basement–bearing middle conglomerate unit, which occurs in all three transects across the southern portion of the Rainbow Gardens Formation basin (Figs. 5A and 10B). We suggest this pulse is also reflected in the detrital zircon data, where the middle conglomerate unit shows an increase in the ca. 1.7 Ga peak (Fig. 8H). The finest-grained, most-distal pulse of this signal is found farthest east, at the Tassi Wash location.

Figure 2 shows the prevalence of Proterozoic basement exposed south of Lake Mead today. Prior to early Miocene volcanism, this basement was widely exposed in the core of the Kingman Uplift. We concur with Beard (1996) and Faulds et al. (2001) that the crystalline basement sediment, for the most part, was largely blocked from the Rainbow Gardens Formation basin by south- and southeast-facing scarps of Permian and older Paleozoic strata (Fig. 10); this is supported by a lack of Proterozoic sediment elsewhere in the Rainbow Gardens Formation strata. South of the paleoscarp, streams drained eastward and westward off of the Kingman Uplift, not northward (Fig. 10A).

We suggest that this scarp, however, was either nonexistent on the west side of the Kingman Uplift (Fig. 1; see location of question marks on Fig. 10) or was breached at some point along its trace (Fig. 10B). First, the paleoscarp may not have extended to the west, or it may have been disrupted on the west side of the Kingman Uplift. Pavlis et al. (2014) proposed that the Gerstley–Nopah Peak thrust (GNPT on Fig. 1; see also Fig. 10), a west-northwest–trending, northeast-directed, Laramide-age thrust fault with a basement-cored ramp anticline they documented in the southeastern Death Valley region, extended southeastward and overprinted the north-northeast–trending Sevier thrusts at about the latitude of Jean, Nevada. The southernmost extent of the Paleozoic autochthonous rocks east of the Sevier thrusts ends at about this latitude as well, perhaps cut off by a hypothetical eastern extension of the Gerstley–Nopah Peak thrust (see Fig. 2). We suggest the Gerstley–Nopah Peak thrust could have extended at least as far east as the Lucy Gray Range, thereby structurally elevating Proterozoic basement south of this trend, disrupting the paleoscarp, and allowing detritus coming off the western side of the Kingman Arch to make an end run around the western end of the paleoscarp. If there was a basement-cored anticline in this location, it also might have been another source, in addition to the Kingman Uplift, for the crystalline basement signal.

Another interpretation is that the paleoscarp may have been breached (Fig. 10B) through headward erosion by streams on the north side of the paleoscarp. This in turn might have led to stream capture, whereby a stream draining part of the Kingman Uplift on the south side of the paleoscarp would change course and drain northward. This would have increased the drainage basin area and streamflow, thus increasing the stream energy, sediment load, and ability to transport coarser material farther into the Rainbow Gardens Formation basin.

Implications of Change in Sedimentation at ca. 19 Ma

We considered and evaluated explanations for the influx of coarser crystalline basement material at ca. 19 Ma and thickness changes in the upper part of the middle unit. Stream capture resulting from headward erosion likely contributed to the abrupt change in sedimentation at the southern margin of the basin at ca. 19 Ma. However, erosion and stream capture alone cannot account for the thickness and other changes in the upper part of the middle unit. The middle unit *above* the middle conglomerate at Horse Spring Ridge section A thickens relative to other sections (Fig. 5C), and it is overall coarser grained than in all other localities across the entire basin (Lamb et al., 2015). The upper part of the middle unit is dominantly volcaniclastic and sourced from the north, and therefore not the result of a breach of the Kingman Uplift to the south. This thickening and coarsening of the upper part of the middle unit, particularly at the Horse Spring Ridge locality, suggest an increase in accommodation space and the presence of a main fluvial channel along the zone of increased subsidence. Experimental data suggest that this can happen where the rate of sediment supply is lower than the rate of creation of accommodation space, thereby attracting fluvial channels to the subsidence maximum (Sheets et al., 2002; Hickson et al., 2005). This interpretation points to a possible tectonic signal controlling sedimentation in the upper part of the middle unit after ca. 19 Ma within the southern portion of the basin.

Further support for a tectonic event at this time derives from possibly syndepositional faulting in the Horse Spring Ridge and Upper Lime Wash localities. Lamb et al. (2015) hypothesized the existence of an unconformity within the middle of Rainbow Gardens Formation deposition and suggested that it might be due to a tectonic event. One line of their evidence was an apparent southward thinning of the stratigraphic package immediately above the ca. 19 Ma middle conglomeratic unit and below the capping limestone at the Horse Spring Ridge locality (Lamb et al., 2015, their figure 11). Subsequent field work has revealed structural complexities at the very southern end of the Horse Spring Ridge and Upper Lime Wash localities in outcrops near the Gold Butte fault to the south (Fig. 5, shown as gaps in section). Mapping is currently under way to test this hypothesis.

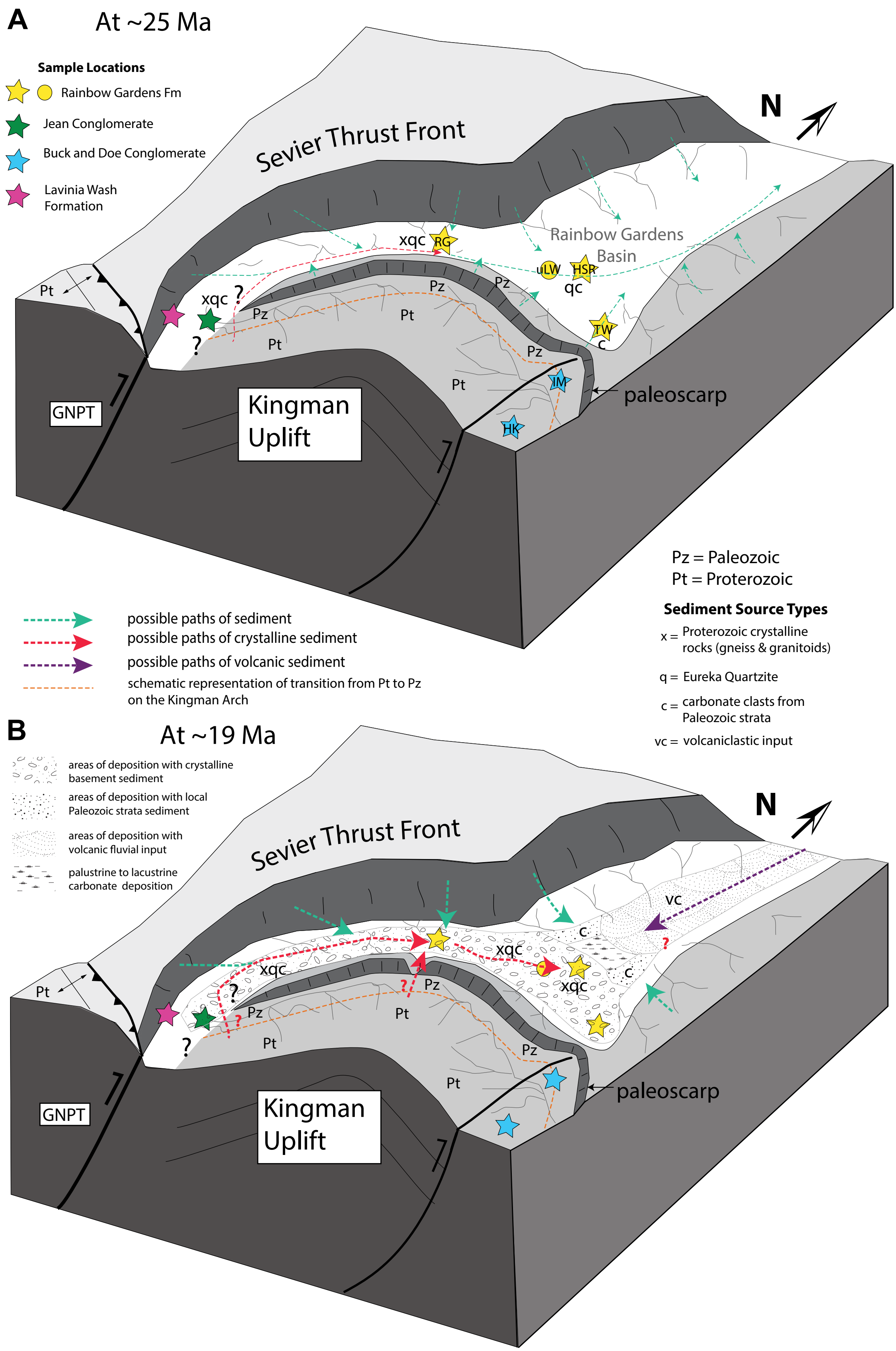

Figure 10. Block diagram showing interpreted paleogeography and sediment pathways. The Sevier uplift and Kingman Uplift north of the paleoscarp of Permian strata provided the majority of sediment throughout deposition of the Rainbow Gardens Formation. Stars show sample locations for detrital zircon analyses; circles indicate field locations without detrital zircon analyses; same location abbreviations as Figure 4. HK—Hackberry Buck and Doe Conglomerate location; RG—Rainbow Gardens; HSR—Horse Spring Ridge; GNPT—Gerstley-Nopah Peak thrust fault of Pavlis et al. (2014). (A) At the start of Rainbow Gardens Formation deposition ca. 25 Ma, a minor crystalline basement (x) component makes it around the paleoscarp of Permian strata to the southwest portion of the basement. (B) At ca. 19 Ma, a major pulse of crystalline basement sediment progrades to the middle of the southern portion of the basement, either from the far southwest or through breaches in the paleoscarp. At this time, volcanic sediment is entering from the north. Note that part B is a time slice between that of T3 and T4 in Lamb et al. (2015).

There are two possible tectonic events that might have been the underlying drivers of these facies changes: initiation of extension or thermal uplift related to volcanism south of Lake Mead. Although extension-related faulting and uplift were clearly under way by 17 Ma based on multiple lines of evidence (e.g., Umhoefer et al., 2010; Fitzgerald et al., 1991, 2009; Reiners et al., 2000; Quigley et al., 2010), thermochronologic data alone suggest extension may have started ca. 20–19 Ma. As mentioned earlier, Quigley et al. (2010) reported a transition from slow cooling beginning 30–26 Ma to rapid cooling at ca. 17 Ma, and Fitzgerald et al. (2009) suggested that cooling may have started 1–2 m.y. before their rapid cooling ages of ca. 17 Ma at Gold Butte and at 18 Ma in the White Hills area. Almeida (2014) reported 20–18 Ma apatite fission-track ages from clasts inferred to be sourced from the Gold Butte block. Finally, Bernet (2002) interpreted that rapid cooling due to the onset of extension began at the Gold Butte block at ca. 21 Ma, based on zircon fission-track data. Changes in sedimentation rates may also suggest extensional activity. Sedimentation rates often reflect faulting: Typical rates in extensional settings vary from 100 to 2000 m/m.y. (Friedmann and Burbank, 1995). Our minimum sedimentation rate for the upper part of the middle unit of the Rainbow Gardens Formation at section A (Fig. 5) of ~116 m/m.y. (Table 2), calculated using the YSG and YC1σ maximum detrital zircon age of the middle conglomeratic unit, suggests active faulting and basin growth. The rate of 73 m/m.y., calculated using the YPP maximum depositional age for the marker unit of 19.6 Ma, is somewhat low for extensional basins but represents an increase above the rate of 24 m/m.y. for the lower part of the middle unit. We recognize that these rates were calculated on fairly thin successions, but, nevertheless, they support the interpretation that the pulse of coarser material across the southern basin at ca. 19 Ma and the stratigraphic observations at section A (coarsest and thickest upper middle unit) may have been due to the initiation of faulting and a resultant change in basin configuration.

Uplift to the south related to the beginning of Cenozoic magmatism is another possible tectonic explanation for the input of coarse clastic material. This magmatism is represented by 19.9–19.6 Ma thin basalt flows exposed more than 60 km south of the White Hills and on the Colorado Plateau margin (Billingsley et al., 2006; Faulds et al., 2001) and by the thick (~1–2 km), ca. 18.5–16 Ma Dixie Queen Mine stratovolcano in the southernmost White Hills, ~75 km SSW of the Horse Spring area (Faulds, 1995; Faulds et al., 2001). Thermal uplift may have increased the regional topographic gradient, creating higher-energy flows that transported coarse-grained sediments farther into the Rainbow Gardens Formation basin.

Climate change can also produce changes in sedimentation as observed at ca. 19 Ma. Globally, the mid-Miocene climatic optimum began at ca. 20–19 Ma, with the cessation of long-term Cenozoic global cooling; this warming continued until ca. 16 Ma, (e.g., Feakins et al., 2012; Ruddiman, 2010). Chapin (2008, and references therein) summarized the major tectonic and oceanic circulation changes that contributed to this global climatic event, as well as the coeval widespread changes in sedimentation across the western United States. Retallack (2007) documented a transition that began ca. 19 Ma to warmer and wetter conditions in Oregon, Montana, and the Great Plains, and Wolfe (1994) pointed to a warming trend in the Pacific Northwest beginning at 20 Ma. Although these more regional comprehensive studies are north and east of the Southwest United States, the mid-Miocene climatic optimum may have also affected the Rainbow Gardens Formation stratigraphy. It may have produced a period of increased precipitation that led to more frequent flooding events. These higher-energy fluvial flows may have extended farther around the southwest margin of the paleoscarp and/or helped create a breach in the paleoscarp. We note, however, that a regional climate event would likely produce higher-energy flows across the region and thus, in turn, produce coarser-grained units on all sides of the basin. We do not see coeval pulses of coarse sediment prograding into basin from other basin margin sites at ca. 19 Ma. Thus, while climate change may have affected Rainbow Gardens Formation sedimentation, we do not think climate change alone can explain the abrupt input of coarse sediment across the southern basin or increase in accommodation space at Horse Spring Ridge.

In summary, we believe that while stream capture and regional climate change may have played a role in the changes in sedimentation documented here and in Lamb et al. (2015), they individually and alone cannot account for all of the changes. We suggest that a tectonic event, either faulting related to extension or thermal uplift relating to volcanism, changed the paleogeography and basin configuration.

Paleogeographic Evolution and Colorado River Implications

We suggest that during and by the end of Sevier thrusting, foreland basin deposits were widespread across the much or all of the Lake Mead area. The ca. 107–93 Ma Lavinia Wash, Willow Tank, and Baseline Sandstone formations were deposited east and southeast of Sevier thrusts that were active up to the early Late Cretaceous (e.g., Keystone, Wilson Cliffs, and Bird Spring thrusts; Garside et al., 2012, and references therein, Burchfiel et al., 1997). Flowers et al. (2008, their figsures 1 and 8) hypothesized that the area near the southern tip of Nevada, west of Kingman, Arizona, had ~1500 m of Late Cretaceous sedimentary strata at 80 Ma; we suggest this extended into the Lake Mead area as well. Erosion of these deposits may have begun with formation of the Kingman Uplift in the Laramide, and they may also have been an additional local source for the Rainbow Gardens Formation, contributing the very weak ca. 100–90 Ma detrital zircon signal.

The various Oligocene–Miocene conglomerates and clastic units deposited across the area share a few key features: They predate extensional deformation, were deposited on older units after a period of erosion, and are locally overlain by volcanic strata. Thus, they all reflect a key time period prior to extension when the regional paleogeography reflecting Sevier thrusting and Laramide uplift was modified by erosion and local deposition. Results of the sandstone provenance, stratigraphic correlations, and detrital zircon analysis support the interpretation of a scarp mostly isolating the Rainbow Gardens

Formation basin from conglomeratic units of the Buck and Doe Conglomerate to the southeast, but connecting to locations to the southwest. Our initial detrital zircon work on the western Jean Conglomerate and eastern Buck and Doe Conglomerate samples suggests they were isolated from each other across the Kingman Uplift (Fig. 10), but additional provenance work is needed to better constrain their relation to each other and create a more complete paleogeographic picture.

The southwestern source for the middle conglomerate unit in the Rainbow Gardens Formation, the strong influx of volcanic material from the north, and the stratigraphic evidence that the southeast part of the Rainbow Gardens Formation basin was distal to both of these sources argue strongly against a major fluvial system entering the basin from the east or transecting the area. Thus, our data do not support the idea of the Rainbow Gardens Formation basin as a sink for paleo–Little Colorado River sediment. Instead, much of the sediment was derived locally, with point sources of volcanic materials from the north and crystalline basement material from the southwest.

CONCLUSIONS

We refined the source areas for the Rainbow Gardens Formation of Lamb et al. (2015) and showed they lay to the south, west, and north. Much of the sediment fill was sourced from the nearby Paleozoic strata, with minor input from possible Mesozoic rocks, and with an influx of volcaniclastic material from the north. Proterozoic clastic material appears to have been sourced from the southwest. Changes in the amount and source of clastic sediment during deposition of the middle unit of the Rainbow Gardens Formation suggest the possibility of tectonic uplift/faulting to the south of Lake Mead ca. 19 Ma as a prelude to major extension at 17 Ma. Provenance data for the southern part of the Rainbow Gardens Formation basin support the conclusion from Lamb et al. (2015) that no paleoriver system flowing westward from the Colorado Plateau entered the basin, but the data do allow for a refinement of the paleogeography. Comparison of the Rainbow Gardens Formation provenance and detrital zircon data with those of conglomeratic units to the south support the idea of a north-facing slope into the southern edge of the basin related to a south-facing paleoscarp and reinforce the location of the Kingman Uplift. These data also lead to the hypothesis that the Lake Mead area was once covered by Sevier thrust–related foreland basin Cretaceous deposits that were subsequently eroded away during the post-Laramide to late Oligocene period of tectonic quiescence.

ACKNOWLEDGMENTS

Funding for much of this work was provided by National Science Foundation grants EAR-0838340 (Lamb and Hickson) and EAR-0838596 (Umhoefer) and the Geology Department at the University of St. Thomas, St. Paul, Minnesota. In addition, National Science Foundation grants EAR-1119629 and EAR-1348007 (University of New Mexico), and EAR-0610103 (University of Nevada–Las Vegas) provided for the detrital zircon analysis, and EAR-1032156 and EAR-1338583 provided support of the Arizona LaserChron Center. The U.S. Geological Survey National Cooperative Geologic Mapping Program provided support for Beard. We thank Bill Dickinson and Mark Pecha for their review of the detrital zircon portion of the paper. We thank the numerous St. Thomas undergraduates who participated in the research during January field work. We specifically thank Crystal Pomerleau, Jay J. Hereford, Michael Payne, and Katrina Korman for field assistance, logistical help, and fruitful discussions. Finally, this paper was greatly improved by thorough reviews by an anonymous reviewer, Jim Faulds, Ernie Anderson, Bob Raynolds, Keith Howard, and Guest Associate Editor Andres Aslan.

REFERENCES CITED

Allmendinger, R., Cardozo, N., and Fisher, D., 2012, Structural Geology Algorithms: Vectors and Tensors in Structural Geology: Cambridge, UK, Cambridge University Press, 304 p.

Almeida, R.V., 2014, Mechanisms and Magnitude of Cenozoic Crustal Extension in the Vicinity of Lake Mead, Nevada, and the Beaver Dam Mountains, Utah: Geochemical, Geochronological, Thermochronological and Geophysical Constraints [Ph.D. thesis]: New York, Columbia University, 362 p.

Anderson, R.E., 1978, Geologic Map of the Black Canyon 15-Minute Quadrangle, Mohave County, Arizona, and Clark County, Nevada: U.S. Geological Survey Geologic Quadrangle Map GQ-1394, scale 1:62,500.

Beard, L.S., 1996, Paleogeography of the Horse Spring Formation in relation to the Lake Mead fault system, Virgin Mountains, Nevada and Arizona, *in* Beratan, K.K., ed., Reconstructing the History of Basin and Range Extension Using Sedimentology and Stratigraphy: Geological Society of America Special Paper 303, p. 27–60, https://doi.org/10.1130/0-8137-2303-5.27.

Beard, L.S., and Faulds, J.E., 2011, Kingman Uplift, paleovalleys and extensional foundering the northwest Arizona, *in* Beard, L.S., Karlstrom, K.E., Young, R.A., and Billingsley, G.H., eds., 2011, CRevolution 2—Origin and Evolution of the Colorado River System, Workshop Abstracts: U.S. Geological Survey Open-File Report 2011–1210, p. 28–37.

Beard, L.S., Anderson, R.E., Block, D.L., Bohannon, R.G., Brady, R.J., Castor, S.B., Duebendorfer, E.M., Faulds, J.E., Felger, T.J., Howard, K.A., Kuntz, M.A., and Williams, V.S., 2007, Preliminary Geologic Map of the Lake Mead 30′ × 60′ Quadrangle, Clark County, Nevada, and Mohave County, Arizona: U.S. Geological Survey Open-File Report 2007–1010, plates 1–3, 109 p.

Bennett, V.C., and DePaolo, D.J., 1987, Proterozoic crustal history of the western United States as determined by neodymium isotopic mapping: Geological Society of America Bulletin, v. 99, p. 674–685, https://doi.org/10.1130/0016-7606(1987)99<674:PCHOTW>2.0.CO;2.

Bernet, M., 2002, Exhuming the Alps Through Time: Clues from Detrital Zircon Fission-Track Ages [M.S. thesis]: New Haven, Connecticut, Yale University, 135 p.

Best, M.G., Christiansen, E.H., Deino, A.L., Gromme, S., Hart, G.L., and Tingey, D.G., 2013, The 36–18 Ma Indian Peak–Caliente ignimbrite field and calderas, southeastern Great Basin, USA: Multicyclic super-eruptions: Geosphere, v. 9, p. 864–950, https://doi.org/10.1130/GES00902.1.

Billingsley, G.H., Block, D.L., and Dyer, J.C., 2006, Geologic Map of the Peach Springs 30′ × 60′ Quadrangle, Mohave and Coconino Counties, Northwestern Arizona: U.S. Geological Survey Scientific Investigations Map I-2900, scale 1:100,000.

Bohannon, R.G., 1984, Nonmarine Sedimentary Rocks of Tertiary Age in the Lake Mead Region, Southeastern Nevada and Northwestern Arizona: U.S. Geological Survey Professional Paper 1259, 72 p.

Burchfiel, B.C., Cameron, C.S., and Royden, L.H., 1997, Geology of the Wilson Cliffs–Potosi Mountain area, southern Nevada: International Geology Review, v. 39, p. 830–854, https://doi.org/10.1080/00206819709465304.

Chapin, C.E., 2008, Interplay of oceanographic and paleoclimate events with tectonism during middle to late Miocene sedimentation across the southwestern USA: Geosphere, v. 4, p. 976–991, https://doi.org/10.1130/GES00171.1.

Crossey, L.C., Karlstrom, K.E., Dorsey, R., Pearce, J., Wan, E., Beard, L.S., Asmerom, Y., Polyak, V., Crow, R.S., Cohen, A., Bright, J., and Pecha, M.E., 2015, Importance of groundwater in propagating downward integration of the 6–5 Ma Colorado River system: Groundwater of springs, travertine and lacustrine carbonates of the Grand Canyon region over the past 12 Ma: Geosphere, v. 11, p. 660–682, https://doi.org/10.1130/GES01073.1.

Davis, S.J., Dickinson, W.R., Gehrels, G.E., Spencer, J.E., Lawton, T.F., and Carroll, A.R., 2010, The Paleogene California River: Evidence of Mojave-Uinta paleodrainager from U-Pb ages of detrital zircons: Geology, v. 38, no. 10, p. 931–934, https://doi.org/10.1130/G31250.1.

Dickinson, W.R., and Gehrels, G.E., 2008, U-Pb ages of detrital zircons in relation to paleogeography: Triassic paleodrainage networks and sediment dispersal across southwest Laurentia: Journal of Sedimentary Research, v. 78, no. 12, p. 745–764, https://doi.org/10.2110/jsr.2008.088.

Dickinson, W.R., and Gehrels, G.E., 2009, Use of U-Pb ages of detrital zircons to infer maximum depositional ages of strata: A test against a Colorado Plateau Mesozoic database: Earth and Planetary Science Letters, v. 288, p. 115–125, https://doi.org/10.1016/j.epsl.2009.09.013.

Dickinson, W.R., Lawton, T.F., Pecha, M., Davis, S.J., Gehrels, G.F., and Young, R.A., 2012, Provenance of the Paleogene Colton Formation (Uinta Basin) and Cretaceous–Paleogene provenance evolution in the Utah foreland: Evidence from U-Pb ages of detrital zircons, paleocurrent trends, and sandstone petrofacies: Geosphere, v. 8, p. 854–880, https://doi.org/10.1130/GES00763.1.

Dickinson, W.R., Karlstrom, K.E., Hanson, A.D., Gehrels, G.F., Pecha, M., Cather, S.M., and Kimbrough, D.L., 2014, Detrital-zircon U-Pb evidence precludes paleo–Colorado River sediment in the exposed Muddy Creek Formation of the Virgin River depression: Geosphere, v. 10, p. 1123–1138, https://doi.org/10.1130/GES01097.1.

Duebendorfer, E.M., Beard, L.S., and Smith, E.I., 1998, Restoration of Tertiary deformation in the Lake Mead region, southern Nevada; the role of strike-slip transfer faults, *in* Faulds, J.E., and Stewart, J.H., eds., Accommodation Zones and Transfer Zones: The Regional Segmentation of the Basin and Range Province: Geological Society of America Special Paper 323, p. 127–148.

Duebendorfer, E.M., Chamberlain, K., and Jones, C.S., 2001, Paleoproterozoic tectonic history of the Cerbat Mountains, northwestern Arizona: Implications for crustal assembly in the southwestern United States: Geological Society of America Bulletin, v. 113, no. 5, p. 575–590, https://doi.org/10.1130/0016-7606(2001)113<0575:PTHOTC>2.0.CO;2.

Faulds, J.E., 1995, Geologic Map of the Mount Davis Quadrangle, Nevada and Arizona: Nevada Bureau of Mines and Geology Map 105, scale 1:24,000 (with accompanying text).

Faulds, J.E., 1996, Geologic Map of the Fire Mountain Quadrangle, Nevada and Arizona: Nevada Bureau of Mines and Geology Map 106, scale 1:24,000 (with accompanying text).

Faulds, J.E., Feuerbach, D.L., Miller, C.F., and Smith, E.I., 2001, Cenozoic evolution of the northern Colorado River extensional corridor, southern Nevada and northwest Arizona, *in* Erskine, M.C., Faulds, J.E., Bartley, J.M., and Rowely, P.D., eds., The Geologic Transition, High Plateaus to Great Basin, the Mackin Symposium: Pacific Section of the American Association of Petroleum Geologists Publication GB 78 (also Utah Geological Association Publication 30), p. 239–272.

Feakins, S.J., Warny, S., and Lee, Jung-Eun, 2012, Hydrologic cycling over Antarctica during the middle Miocene warming: Nature Geoscience, v. 5, p. 557–560, https://doi.org/10.1038/ngeo1498.

Ferguson, C.A., McIntosh, W.C., and Miller, C.F., 2013, Silver Creek caldera—The tectonically dismembered source of the Peach Spring Tuff: Geology, v. 41, no. 1, p. 3–6, https://doi.org/10.1130/G33551.1.

Fitzgerald, P.G., Fryxell, J.E., and Wernicke, B.P., 1991, Miocene crustal extension and uplift in southeastern Nevada; constraints from fission track analysis: Geology, v. 19, p. 1013–1016, https://doi.org/10.1130/0091-7613(1991)019<1013:MCEAUI>2.3.CO;2.

Fitzgerald, P.G., Duebendorfer, E.M., Faulds, J.E., and O'Sullivan, P., 2009, South Virgin–White Hills detachment fault system of SE Nevada and NW Arizona: Applying apatite fission track thermochronology to constrain the tectonic evolution of a major continental detachment fault: Tectonics, v. 28, TC2001, https://doi.org/10.1029/2007TC002194.

Fleck, R.J., 1970, Tectonic style, magnitude, and age of deformation in the Sevier orogenic belt in southern Nevada and eastern California: Geological Society of America Bulletin, v. 81, p. 1705–1720, https://doi.org/10.1130/0016-7606(1970)81[1705:TSMAAO]2.0.CO;2.

Flowers, R.M., and Farley, K.A., 2012, Apatite ^{4}He/^{3}He and (U-Th)/He evidence for an ancient Grand Canyon: Science, v. 338, p. 1616–1619, https://doi.org/10.1126/science.1229390.

Flowers, R.M., Wernicke, B.P., and Farley, K.A., 2008, Unroofing, incision and uplift history of the southwestern Colorado Plateau from apatite (U-Th)/He thermochronometry: Geological Society of America Bulletin, v. 120, p. 571–587, https://doi.org/10.1130/B26231.1.

Friedmann, S.J., and Burbank, D.W., 1995, Rift basins and supradetachment basins: Intracontinental extensional end-members: Basin Research, v. 7, p. 109–127, https://doi.org/10.1111/j.1365-2117.1995.tb00099.x.

Fryxell, J.E., and Duebendorfer, E.M., 2005, Origin and trajectory of the Frenchman Mountain block, an extensional allochthon in the Basin and Range Province, southern Nevada: The Journal of Geology, v. 113, p. 355–371, https://doi.org/10.1086/428810.

Garside, L.J., House, P.K., Burchfiel, B.C., Rowland, S.M., and Buck, B., 2012, Geologic Map of the Jean Quadrangle, Clark County, Nevada: Nevada Bureau of Mines and Geology Map 176, scale 1:24,000.

Gehrels, G.E., Blakey, R., Karlstrom, K.E., Timmons, J.M., Dickinson, B., and Pecha, M., 2011, Detrital zircon U-Pb geochronology of Paleozoic strata in the Grand Canyon, Arizona: Lithosphere, v. 3, p. 183–200, https://doi.org/10.1130/L121.1.

Goldstrand, P.M., 1992, Evolution of Late Cretaceous and early Tertiary basins of southwest Utah based on clastic petrology: Journal of Sedimentary Petrology, v. 62, p. 495–507.

Hanson, A.D., 2008, Detrital zircon constraints on the Jean conglomerate and Sevier unroofing near Las Vegas: Geological Society of America Abstracts with Programs, v. 40, no. 1, p. 56.

Herrington, J.M., 1993, Evolution of the Kingman Arch [M.S. thesis]: Las Vegas, Nevada, University of Nevada–Las Vegas, 82 p.

Hickson, T.A., Sheets, B.A., Paola, C., and Kelberer, M., 2005, Experimental test of tectonic controls on three-dimensional alluvial facies architecture: Journal of Sedimentary Research, v. 75, p. 710–722, https://doi.org/10.2110/jsr.2005.057.

Hinz, N.H., Ramelli, A.R., and Dee, S., 2015, Preliminary Geologic Map of the Sloan Quadrangle, Clark County, Nevada: Nevada Bureau of Mines and Geology Open-File Report 15–7, scale 1:24,000.

House, P.K., Ramelli, A.R., and Buck, B.J., 2006, Surficial Geologic Map of the Ivanpah Valley Area, Clark County, Nevada: Nevada Bureau of Mines and Geology Map 156, scale 1:50,000.

Karlstrom, K., Lee, J., Kelley, S., Crow, R., Young, R., Lucchitta, I., Beard, S., Dorsey, R., Ricketts, J., Dickinson, W., and Crossey, L., 2013, Comment on "Apatite ^{4}He/^{3}He and (U-Th)/He Evidence for an Ancient Grand Canyon": Science, v. 340, p. 143, https://doi.org/10.1126/science.1233982.

Karlstrom, K.E., Lee, J.P., Kelley, S.A., Crow, R.S., Crossey, L.J., Young, R.A., Lazear, G., Beard, L.S., Ricketts, J.W., Fox, M., and Shuster, D.L., 2014, Formation of the Grand Canyon 5 to 6 million years ago through integration of older palaeocanyons: Nature Geoscience, v. 7, p. 239–244, https://doi.org/10.1038/ngeo2065.

Karlstrom, K.E., Crossey, L.J., Embid, E., Crow, R., Heizler, M., Hereford, R., Beard, L.S., Ricketts, J.W., Cather, S., Kelley, S., 2017, Cenozoic incision history of the Little Colorado River: Its role in carving Grand Canyon and onset of rapid incision in the last ~2 Ma in the Colorado River system: Geosphere, CRevolution volume, v. 13, no. 1, p. 49–81, doi:10.1130/GES01304.1.

Lamb, M., Umhoefer, P.J., Anderson, E.A., Beard, L.S., Hickson, T., and Martin, L.K., 2005, Development of Miocene faults and basins in the Lake Mead region: A tribute to Ernie Anderson and a review of new research on basins, *in* Pederson, J.L., and Dehler, C.M., eds., Interior Western United States: Geological Society of America Field Guide 6, p. 389–418, https://doi.org/10.1130/2005.fld006(18).

Lamb, M., Beard, L.S., Hickson, T., Umhoefer, P., Dunbar, N., Schleicher, J., and McIntosh, W., 2015, Sedimentation and paleogeography at the onset of extension in the central Basin and Range, Lake Mead area: Rainbow Gardens Formation of the Oligo-Miocene Horse Spring Formation: Geological Society of America Bulletin, v. 127, p. 899–925, https://doi.org/10.1130/B31144.1.

Larsen, J.S., Link, P.K., Roberts, E.M., Tapanila, L., and Fanning, C.M., 2010, Cyclic stratigraphy of the Paleogene Pine Hollow Formation and detrital zircon provenance of the Campanian to Eocene sandstones of the Kaiparowits and Table Cliffs basins, south-central Utah, *in* Carney, S.M., Tabet, D.E., and Johnson, C.L., eds., Geology of South-Central Utah: Utah Geological Association Publication 39, p. 194–224.

Lee, J.P., Stockli, D.F., Kelley, S.A., Pederson, J.L., Karlstrom, K.E., and Ehlers, T.A., 2013, New thermochronometric constraints on the Tertiary landscape evolution of central and eastern Grand Canyon, Arizona: Geosphere, v. 9, no. 2, p. 216–228, https://doi.org/10.1130/GES00842.1.

Lucchitta, I., 1966, Cenozoic Geology of the Upper Lake Mead Area Adjacent to the Grand Wash Cliffs, Arizona [Ph.D. dissert.]: University Park, Pennsylvania, Pennsylvania State University, 218 p.

Lucchitta, I., and Young, R.A., 1986, Structure and geomorphic character of western Colorado Plateau in the Grand Canyon–Lake Mead region, *in* Nations, J.D., Conway, C.M., and Swann, G.A., eds., Geology of Central and Northern Arizona: Flagstaff, Arizona, Northern Arizona University, and Geological Society of America, Rocky Mountain Section Guidebook, p. 159–176.

Ludington, S., Moring, B.C., Miller, R.J., Stone, P.A., Bookstrom, A.A., Bedford, D.R., Evans, J.G., Haxel, G.A., Nutt, C.J., Flyn, K.S., and Hopkins, M.J., 2007, Preliminary Integrated Geologic Map Databases for the United States, Western States: California, Nevada, Arizona, Washington, Oregon, Idaho, and Utah, Version 1.3: U.S. Geological Survey Open-File Report 2005–1305, 47 p., https://pubs.usgs.gov/of/2005/1305/.

Pape, D.E., Spell, T.L., Bonde, J.W., Fish, B., and Rowland, S.M., 2011, ^{40}Ar/^{39}Ar isotopic dates for the fossiliferous Willow Tank Formation (Cretaceous) in Valley of Fire State Park, Nevada: Geological Society of America Abstracts with Programs, v. 43, no. 5, p. 586.

Pavlis, T., Rutkofske, J., Guerrero, F., and Serpa, L., 2014, Structural overprinting of Mesozoic thrust systems in eastern California and its importance to reconstruction of Neogene extension in the southern Basin and Range: Geosphere, v. 10, p. 732–756, https://doi.org/10.1130/GES00993.1.

Pederson, J.L., 2008, The mystery of the pre–Grand Canyon Colorado River; results from the Muddy Creek Formation: GSA Today, v. 18, no. 3, p. 4–10, https://doi.org/10.1130/GSAT01803A.1.

Quigley, M.C., Karlstrom, K.E., Kelley, S., and Heizler, J., 2010, Timing and mechanisms of basement uplift and exhumation in the Colorado Plateau–Basin and Range transition zone, Virgin Mountain anticline, Nevada-Arizona, *in* Umhoefer, P.J., Lamb, M.A., and Beard, L.S., eds., Miocene Tectonics of the Lake Mead Region: Geological Society of America Special Paper 463, p. 311–329, https://doi.org/10.1130/2010.2463(14).

Reiners, P.W., Brady, R., Farley, K.A., Fryxell, J.E., Wernicke, B., and Lux, D., 2000, Helium and argon thermochronometry of the Gold Butte block, south Virgin Mountains, Nevada: Earth and Planetary Science Letters, v. 178, p. 315–326, https://doi.org/10.1016/S0012-821X(00)00080-7.

Retallack, G.J., 2007, Cenozoic paleoclimate on land in North America: The Journal of Geology, v. 115, p. 271–294, https://doi.org/10.1086/512753.

Rice, J.A., 1987, Sedimentology, Provenance, and Tectonic Significance of the Basal Conglomerate of the Rainbow Gardens Formation of the Miocene Horse Spring Formation, Lake Mead Area, Southeastern Nevada [M.S. thesis]: Las Vegas, Nevada, University of Nevada–Las Vegas, 171 p.

Ruddiman, W.F., 2010, A paleoclimate enigma?: Science, v. 328, p. 838–839, https://doi.org/10.1126/science.1188292.

Schmidt, M.J., 2014, Structural and Basin Evolution of the Mud Hills, Lake Mead Miocene Extensional Domain, Nevada, [M.S. thesis]: Flagstaff, Arizona, Northern Arizona University, 176 p.

Sheets, B., Hickson, T., and Paola, C., 2002, Assembling the stratigraphic record: Depositional patterns and time-scales in an experimental alluvial basin: Basin Research, v. 14, p. 287–301, https://doi.org/10.1046/j.1365-2117.2002.00185.x.

Stewart, J.H., 1998, Regional characteristics, tilt domains, and extensional history of the later Cenozoic Basin and Range Province, western North America, *in* Faulds, J.E., and Stewart, J.H., eds., Accommodation Zones and Transfer Zones: The Regional Segmentation of the Basin and Range Province: Geological Society of America Special Paper 323, p. 47–74, https://doi.org/10.1130/0-8137-2323-X.47.

Troyer, B.R, Barth, A.P., Wooden, J.L., and Jacobson, C., 2006, Provenance and timing of Sevier foreland basin sediments in the Valley of Fire, southern Nevada, from U-Pb geochronology [abs.]: Geological Society of America Abstracts with Programs, v. 38, no. 7, p. 369.

Umhoefer, P.J., Beard, L.S., Martin, K.L., and Blythe, N., 2010, From detachment to transtensional faulting: A model for the Lake Mead extensional domain based on new ages and correlation of subbasins, *in* Umhoefer, P.E., Lamb, M.A., and Beard, L.S., eds., Miocene Tectonics of the Lake Mead Region, Central Basin and Range: Geological Society of America Special Paper 463, p. 371–394, https://doi.org/10.1130/2010.2463(17).

Wells, M.L., 2016, A major mid-Cretaceous shortening event in the southern Sevier orogenic belt: Continental record of global plate reorganization?: Geological Society of America Abstracts with Programs, v. 48, no. 7, paper no. 143-11, https://doi.org/10.1130/abs/2016AM-287809.

Wernicke, B.P., 2011, The California River and its role in carving Grand Canyon: Geological Society of America Bulletin, v. 123, p. 1288–1316, https://doi.org/10.1130/B30274.1.

Wernicke, B.P., Axen, G.J., and Snow, J.K., 1988, Basin and Range extensional tectonics at the latitude of Las Vegas, Nevada: Geological Society of America Bulletin, v. 100, p. 1738–1757, https://doi.org/10.1130/0016-7606(1988)100<1738:BARETA>2.3.CO;2.

Winn, C., Karlstrom, K.E., Shuster, D., Kelley, S., and Fox, M., 2017, 6 Ma age of carving westernmost Grand Canyon: Reconciling geologic data with combined AFT, (U-Th)/He, and ^{4}He/^{3}He thermochronologic data: Earth and Planetary Science Letters, v. 474, p. 257–271, http://dx.doi.org/10.1016/j.epsl.2017.06.051.

Wolfe, J., 1994, Tertiary climatic changes at middle latitudes of western North America: Palaeogeography, Palaeoclimatology, Palaeoecology, v. 108, p. 195–205, https://doi.org/10.1016/0031-0182(94)90233-X.

Young, R.A., 1979, Laramide deformation, erosion and plutonism along the southwestern margin of the Colorado Plateau: Tectonophysics, v. 61, p. 25–47, https://doi.org/10.1016/0040-1951(79)90290-7.

Young, R.A., 1985, Geomorphic evolution of the Colorado Plateau margin in west-central Arizona; a tectonic model to distinguish between the causes of rapid symmetrical scarp retreat and scarp dissection, *in* Hack, J.T., and Morisawa, M., eds., Tectonic Geomorphology: Binghamton Symposia in Geomorphology International Series 15: London, Allen and Unwin, p. 261–278.

Young, R.A., 1999, Nomenclature and ages of Late Cretaceous(?)–Tertiary strata in the Hualapai Plateau region, northwest Arizona, *in* Billingsley, G.H., Wenrich, K.J., Huntoon, P.W., and Young, R.A., eds., Breccia Pipe and Geologic Map of the Southwestern 1162 Part of the Hualapai Indian Reservation and Vicinity, Arizona: U.S. Geological Survey Miscellaneous Investigations Series Map I-2554, scale 1:48,000, Appendix, p. 21–50.

Young, R.A., 2001, Geomorphic, structural, and stratigraphic evidence for Laramide uplift of the southwestern Colorado Plateau margin in northwestern Arizona, *in* Erskine, M.C., Faulds, J.E., Bartley, J.M., and Rowley, P.D., eds., The Geologic Transition Colorado Plateau to Great Basin—A Symposium and Field Guide (The Mackin Volume): Utah Geological Association Publication 30, p. 227–237.

Young, R.A., and Brennan, W.J., 1974, Peach Springs Tuff: Its bearing on structural evolution of the Colorado Plateau and development of Cenozoic drainage in Mohave County, Arizona: Geological Society of America Bulletin, v. 85, p. 83–90, https://doi.org/10.1130/0016-7606(1974)85<83:PSTIBO>2.0.CO;2.

Young, R.A., and Crow, R., 2014, Paleogene Grand Canyon incompatible with Tertiary paleogeography and stratigraphy: Geosphere, v. 10, p. 664–679, https://doi.org/10.1130/GES00973.1.

Young, R.A., and Hartman, J.H., 2014, Paleogene rim gravel of Arizona: Age and significance of the Music Mountain Formation: Geosphere, v. 10, p. 870–891, https://doi.org/10.1130/GES00971.1.